© 2019. Published by The Company of Biologists Ltd | Journal of Cell Science (2019) 132, jcs227165. doi:10.1242/jcs.227165

RESEARCH ARTICLE

Distinct functions of a cGMP-dependent protein kinase in nerve terminal growth and synaptic vesicle cycling

Jeffrey S. Dason[1,2,‡], Aaron M. Allen[1,*], Oscar E. Vasquez[3] and Marla B. Sokolowski[1,3,4,‡]

ABSTRACT

Sustained neurotransmission requires the tight coupling of synaptic vesicle (SV) exocytosis and endocytosis. The mechanisms underlying this coupling are poorly understood. We tested the hypothesis that a cGMP-dependent protein kinase (PKG), encoded by the *foraging* (*for*) gene in *Drosophila melanogaster*, is critical for this process using a *for* null mutant, genomic rescues and tissue-specific rescues. We uncoupled the exocytic and endocytic functions of FOR in neurotransmission using a temperature-sensitive *shibire* mutant in conjunction with fluorescein-assisted light inactivation of FOR. We discovered a dual role for presynaptic FOR, in which FOR inhibits SV exocytosis during low-frequency stimulation by negatively regulating presynaptic Ca^{2+} levels and maintains neurotransmission during high-frequency stimulation by facilitating SV endocytosis. Additionally, glial FOR negatively regulated nerve terminal growth through TGF-β signalling, and this developmental effect was independent of the effects of FOR on neurotransmission. Overall, FOR plays a critical role in coupling SV exocytosis and endocytosis, thereby balancing these two components to maintain sustained neurotransmission.

KEY WORDS: Exocytosis, Endocytosis, Synaptic transmission, Presynaptic, Neurotransmitter release

INTRODUCTION

Neurotransmission is essential for proper nervous system function. Chemical neurotransmission involves the fusion of synaptic vesicles (SVs) with the presynaptic plasma membrane and the release of neurotransmitter molecules (exocytosis). Subsequently, SV components are retrieved from the plasma membrane and SVs are re-formed (endocytosis). Maintaining a balance between SV exocytosis and endocytosis requires a tight coupling of these two processes, which is critical for sustained synaptic transmission (Haucke et al., 2011; Wu et al., 2014; Soykan et al., 2016). However, the mechanisms underlying this coupling have largely remained elusive. Presynaptic Ca^{2+} (Hosoi et al., 2009), and Synaptotagmin (Syt) (Poskanzer et al., 2003; Yao et al., 2012) and SNARE (Deák et al., 2004; Xu et al., 2013; Zhang et al., 2013) proteins are thought to be involved in coupling SV exocytosis and endocytosis. Many presynaptic proteins that regulate SV exocytosis and endocytosis undergo phosphorylation/dephosphorylation (Turner et al., 1999; Clayton et al., 2007; Kohansal-Nodehi et al., 2016). Changes in phosphorylation state can alter the affinity of proteins for some of their binding partners (Clayton et al., 2009; Cho et al., 2015; Geng et al., 2016), as well as alter the probability of ion channels opening (Huang and Zamponi, 2017). Kinases are thus compelling candidates for involvement in the coupling of SV exocytosis and endocytosis.

Kinases are multifaceted by nature and regulate a wide variety of cellular processes (Jordán-Álvarez et al., 2012; Chen et al., 2014; Piccioli and Littleton, 2014; Zhao et al., 2015; Spring et al., 2016; Krill and Dawson-Scully, 2016; Cantarutti et al., 2018). In the nervous system, a single kinase can affect multiple developmental and physiological processes. Consequently, pharmacological and genetic approaches have been unable to determine whether a given kinase affects the coupling of SV exocytosis and endocytosis or only one with concomitant effects on the other. To understand their role in synaptic function it is critical to be able to inactivate kinases with high spatiotemporal resolution.

Optogenetic approaches have recently been used to acutely activate kinases (Krishnamurthy et al., 2016; O'Banion et al., 2018). However, acute inactivation of an endogenously expressed kinase has not been achieved to date. Fluorescein-assisted light inactivation (FALI) has been used to acutely inactivate proteins at the *Drosophila* larval neuromuscular junction (NMJ) within minutes, and bypass any lethality and developmental effects of these proteins (Marek and Davis, 2002; Kasprowicz et al., 2008, 2014; Heerssen et al., 2008; Vanlandingham et al., 2014). Furthermore, the *Drosophila* dynamin [*shibire* (*shi*)] mutant, *shibire-ts1*, can be used to uncouple SV exocytosis and endocytosis; this mutant undergoes reversible, temperature-sensitive endocytic blockade and can be used to trap SVs on the plasma membrane following SV fusion (Koenig and Ikeda, 1989; Ramaswami et al., 1994). FALI has been used in conjunction with SV trapping to test the function of Syt1 in SV endocytosis following normal stimulus-dependent exocytosis (Poskanzer et al., 2003).

Here, we use this approach to investigate the functions of a cGMP-dependent protein kinase (PKG) at the synapse. PKGs are good candidates to be involved in coupling SV exocytosis and endocytosis because they are thought to affect both processes (Yawo, 1999; Luo et al., 2012; Eguchi et al., 2012; Taoufiq et al., 2013; Collado-Alsina et al., 2014). However, these two processes are intricately linked at the synapse, making it possible that the reported effects of a PKG on one process could be due to concomitant effects on the other. In addition, PKGs have also been reported to have a developmental role that involves regulating axon guidance and growth (Peng et al., 2016; Sild et al., 2016). Whether the effects of a PKG on SV exocytosis and endocytosis are interrelated or distinct from these developmental effects has not been determined. Furthermore, presynaptic, postsynaptic and glial

[1]Department of Cell and Systems Biology, University of Toronto, Toronto, ON M5S 3B2, Canada. [2]Department of Biological Sciences, University of Windsor, Windsor, ON N9B 3P4, Canada. [3]Department of Ecology and Evolutionary Biology, University of Toronto, Toronto, ON M5S 3B2, Canada. [4]Child and Brain Development Program, Canadian Institute for Advanced Research (CIFAR), Toronto, ON M5G 1M1, Canada.
*Present address: Centre for Neural Circuits and Behaviour, University of Oxford, Oxford OX1 3SR, UK.

‡Authors for correspondence (jeffrey.dason@uwindsor.ca; marla.sokolowski@utoronto.ca)

J.S.D., 0000-0002-5499-0156; M.B.S., 0000-0002-7462-8007

Received 1 November 2018; Accepted 26 February 2019

Journal of Cell Science (2019) 132, jcs227165. doi:10.1242/jcs.227165

PKGs may all contribute to these synaptic effects. Thus, a PKG at the synapse may have several distinct temporal and spatial functions. To investigate this, we tagged the *Drosophila foraging* (*for*) gene, which encodes a PKG orthologue of the mammalian *Prkg1* gene (Osborne et al., 1997), for 4′,5′-bis[1,3,2-dithioarsolan-2-yl] fluorescein (FlAsH)-mediated FALI (FlAsH-FALI), and show that FOR does have multiple separable functions at the synapse.

RESULTS

The *Drosophila* larval NMJ is a well-established preparation for studying nerve terminal growth and SV cycling (Harris and Littleton, 2015). To determine whether FOR was expressed at the larval NMJ, we used recombineering to generate a bacterial artificial chromosome (BAC) containing the entire *for* locus with a flag-4c tag on the C-terminus (Fig. 1A). We expressed this BAC in a *for* null background. The C-terminus was tagged because it is common to all FOR isoforms (Allen et al., 2017; Fig. 1A). Western blot analysis showed that $+;for^{0};\{for^{flag\text{-}4c}\}$ larvae had similar levels of FOR to wild-type larvae (Fig. 1B,C). To visualize FOR expression at the NMJ of muscle fibres 6 and 7, mid-third-instar larvae expressing FOR-flag-4c under endogenous *for* promoter control were stained with an anti-flag antibody. These muscles are innervated by two types of axons that result in type 1b and type 1s boutons, which differ in both their morphological and physiological properties (Kurdyak et al., 1994). We found FOR enriched in both 1b and 1s boutons (Fig. 1D,F) and colocalized with the presynaptic cytoplasmic protein Complexin (Cpx) (Fig. 1G) and the plasma membrane marker horseradish peroxidase (HRP) (Fig. 1H). No obvious signal was observed in muscles (Fig. 1D). As expected, control larvae without the flag tag showed no anti-flag staining (Fig. 1E). FOR was also present in glia (Fig. 1D), and this signal overlapped with GFP driven by a glial driver, *46F-GAL4* (Brink et al., 2012; Fig. 1I). To further confirm that FOR is expressed in glia at the larval NMJ we examined several promoter-driven *for-GAL4* drivers (Allen et al., 2018). Four GAL4 lines were previously generated by cloning regions surrounding the four transcription start sites of the *for* gene (Allen et al., 2018). We found that one expressed strongly in glia at the NMJ (Fig. S1A,B) and this was confirmed by co-staining for the glial marker Gliotactin (Gli) (Fig. S1C). No presynaptic bouton expression was seen with any of the promoter-driven *for-GAL4* drivers. This is likely because the cloned regions used for the promoter-driven *for-GAL4* drivers likely do not encapsulate all of the regulatory elements from the *for* locus, as together they covered less than half of the gene. Collectively, these data show that the *Drosophila* NMJ is an ideal preparation for dissecting the role(s) of FOR in nerve terminal growth and SV cycling, as FOR is found in presynaptic boutons and glia.

Glial FOR negatively regulates nerve terminal growth

To investigate the role of FOR in nerve terminal growth, we stained NMJs from muscle fibres 6 and 7 of abdominal segment 3 from mid-third-instar larvae with anti-HRP (a neuronal membrane marker) and anti-Bruchpilot (BRP; an active zone marker; Wagh et al., 2006) antibodies. The number of 1b and 1s boutons was significantly increased in the for^{0} null mutant in comparison to control and genomic rescue larvae (Fig. 2A,B). The number of active zones per bouton, estimated by counting the number of BRP spots from a sample of 1b boutons (~5µm in diameter) and 1s boutons (~2µm in diameter), was not different in the for^{0} null mutant in comparison to control and genomic rescue larvae (Fig. 2C,D). We conclude from these data that FOR negatively regulates nerve terminal growth at the NMJ, but does not affect the number of active zones per bouton.

To determine whether presynaptic, postsynaptic (muscle) or glial FOR was required for nerve terminal growth, we used the GAL4/UAS system (Brand and Perrimon, 1993) to perform tissue-specific

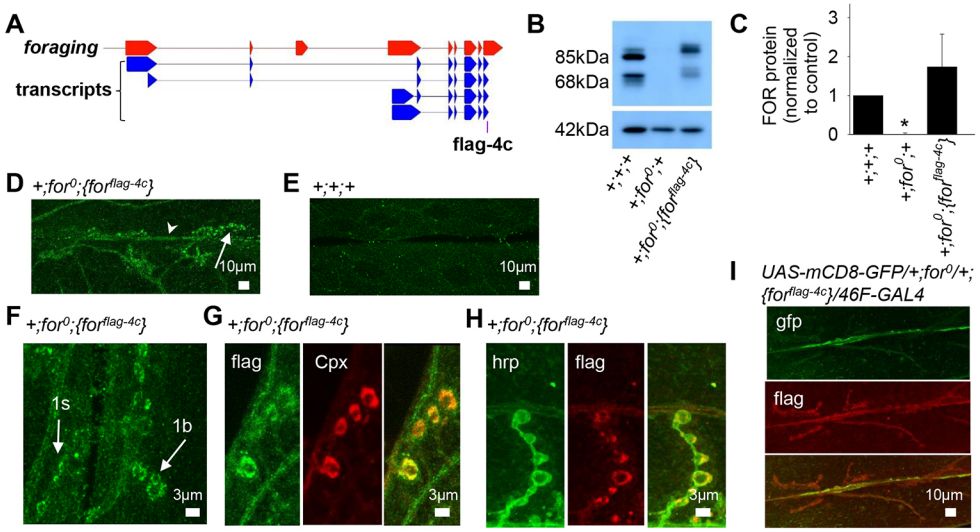

Fig. 1. FOR is expressed at the larval NMJ. (A) Schematic of $for^{flag\text{-}4c}$ allele tagged with a flag tag and a FALI-sensitive tetracysteine (4c) cassette on the C-terminus. Gene structure of *for* in red. Coding exons of *for* are in blue and flag-4c is in purple. The C-terminus was chosen because it is common to all FOR isoforms. A BAC containing $for^{flag\text{-}4c}$ was incorporated into the fly's genome using ϕC31 integration into the attP2 landing site on the third chromosome. (B,C) Western blot of whole larval homogenates of control (+;+;+), *for* null (+;for^{0};+) and rescue (+;for^{0};{$for^{flag\text{-}4c}$}) genotypes (B). Note that $for^{flag\text{-}4c}$ expresses FOR protein in a for^{0} null mutant background. A monoclonal anti-actin antibody was used as a loading control. Four biological replicates were performed for all genotypes. No significant differences in FOR protein levels were found between the control and rescue genotypes ($P>0.05$) (C). There was significant reduction in FOR protein levels in the for^{0} null mutant (*$P<0.05$). Values represent the mean±s.e.m. Significance was determined using one-way ANOVA. (D–F) Representative images of fixed third-instar larval NMJs stained with an anti-flag antibody. (D) +;for^{0};{$for^{flag\text{-}4c}$} NMJs display expression in presynaptic boutons (arrows) and glia (arrowhead). (E) No staining was observed in control NMJs. (F) Representative zoomed-in images of 1b and 1s boutons in +;for^{0};{$for^{flag\text{-}4c}$} NMJs. (G,H) FOR-flag-4c expression colocalizes with anti-Cpx (G) and anti-HRP (H). (I) FOR-flag-4c expression also colocalizes with GFP driven by the glial driver *46F-GAL4*.

Journal of Cell Science (2019) 132, jcs227165. doi:10.1242/jcs.227165

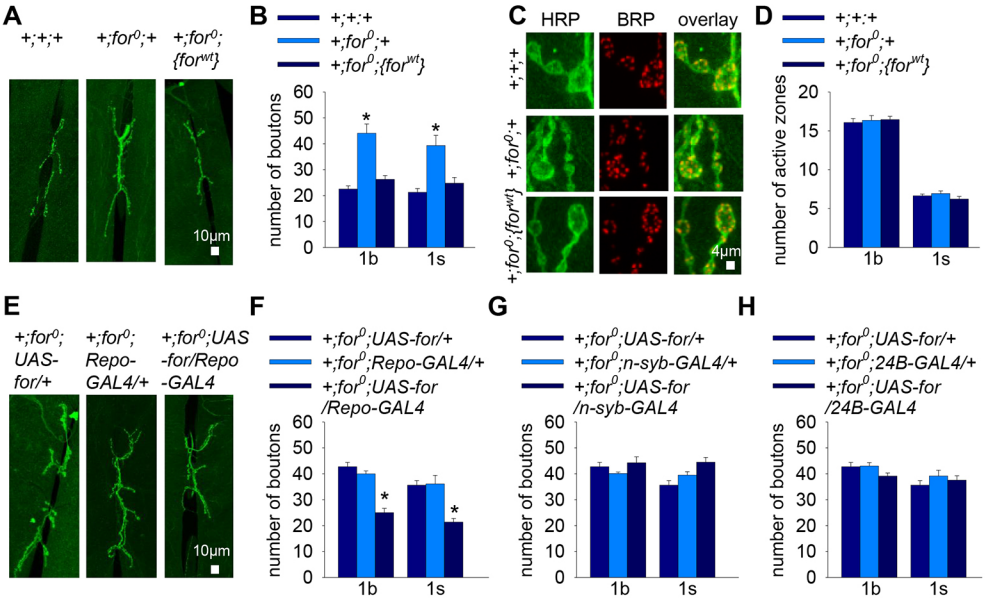

Fig. 2. Glial FOR negatively regulates nerve terminal growth. (A,E) Fixed larval NMJs stained with FITC-conjugated anti-HRP antibody. (B) The number of 1b and 1s boutons was significantly increased in *for*^{0} null mutants (+;*for*^{0};+, *n*=12) in comparison to control (+;+;+, *n*=11) and genomic rescue (+;*for*^{0};{*for*^{wt}}, *n*=11) genotypes (**P*<0.001 for 1b boutons and **P*=0.001 for 1s boutons). (C) Representative images of 1b and 1s boutons stained with FITC-conjugated anti-HRP antibody and anti-BRP. (D) The number of active zones per 1b or 1s bouton was not significantly different between *for*^{0} null mutants (+;*for*^{0};+, *n*=14), controls (+;+;+, *n*=14) and genomic rescue (+;*for*^{0};{*for*^{wt}}, *n*=18) genotypes (*P*=0.865 for 1b boutons and *P*= 0.274 for 1s boutons). (F) The increased number of 1b and 1s boutons seen in the *for*^{0} null mutant was rescued by FOR expression in glia (+;*for*^{0};*UAS-for-flag-4c*/*Repo-GAL4*, *n*=11), whereas in *UAS-for* (+;*for*^{0};*UAS-for-flag-4c*/+, *n*=8) or *Repo-GAL4* (+;*for*^{0};*Repo-GAL4*/+, *n*=10) controls, there was no rescue of the increased nerve terminal growth seen in the *for*^{0} null mutants (**P*<0.001 for 1b and 1s boutons; *n*=8–11). (G,H) The increased number of 1b and 1s boutons seen in the *for*^{0} null mutant was not rescued by FOR expression in neurons (*P*>0.05; *n*=8) or muscles (*P*>0.05; *n*=7). Values represent the mean±s.e.m. Significance was determined using one-way ANOVA.

rescues. To accomplish this, we generated transgenic flies to express FOR with a flag-4c tag on the C-terminus (*UAS-for-flag-4c*) in selective tissues. When *UAS-for-flag-4c* was driven by the ubiquitous GAL4 driver, *da-GAL4*, FOR expression was increased (Fig. S2A). Using tissue-specific GAL4s, we selectively drove FOR expression presynaptically (*n-syb-GAL4*; Fig. S2B,C), postsynaptically (*24B-GAL4*; Fig. S2D) or in glia (*Repo-GAL4*; Fig. S2E) at the larval NMJ. We defined a rescue as being not significantly different from wild type, but significantly different from larvae that express the GAL4 and larvae that express the UAS transgene in a *for*^{0} null mutant background. Expression of FOR in glia in a *for*^{0} null mutant background was sufficient to rescue the increased nerve terminal growth seen in *for*^{0} null mutants (Fig. 2E,F). In contrast, presynaptic (Fig. 2G) or postsynaptic (Fig. 2H) expression of FOR did not rescue the increased nerve terminal growth seen in *for*^{0} null mutants. Together, these data show that FOR acts in glia to negatively regulate nerve terminal growth at the NMJ.

Glia at the *Drosophila* NMJ are known to release Maverick (Mav), a TGF-β ligand that regulates nerve terminal growth (Fuentes-Medel et al., 2012). We hypothesized that FOR functions through Mav to regulate nerve terminal growth. We knocked down glial Mav in a *for*^{0} null mutant background and found that this rescued the increased nerve terminal growth seen in *for*^{0} null mutants (Fig. 3A,B). Mav is thought to control the release of the *Drosophila* TGF-β/BMP homologue, Glass bottom boat (Gbb), from muscles, which fine-tunes the ability of motor neurons to extend new synaptic boutons (Fuentes-Medel et al., 2012). We hypothesized that if FOR was acting through Mav, then knocking down muscle Gbb would also rescue the increased nerve terminal growth seen in *for*^{0} null mutants. As we predicted, knocking down Gbb in muscles rescued the increased nerve terminal growth seen in *for*^{0} null mutants (Fig. 3C,D). We also reduced expression of Gbb in glia and found that it did not rescue the increased nerve terminal growth seen in *for*^{0} null mutants (Fig. S3A,B). Thus, FOR acts in glia to negatively regulate nerve terminal growth, likely through a pathway that involves glial Mav and muscle Gbb.

FOR negatively regulates neurotransmitter release and presynaptic Ca^{2+} levels in response to low-frequency stimulation

We next assessed the role of FOR in neurotransmitter release by recording the compound excitatory junction potential (EJP) generated by tonic-like type 1b and phasic-like type 1s boutons from segment 3 of muscle fibre 6 in mid-third-instar larvae in HL6 saline (0.5 mM Ca^{2+}) in response to low-frequency stimulation (0.05 Hz). We found a significant increase in EJP amplitude in *for*^{0} null mutants compared to control and genomic rescue larvae (Fig. 4A,B), showing that FOR affects evoked neurotransmitter release. There was no significant difference in miniature excitatory junction potential (mEJP) amplitude (Fig. 4A,C). There was a mild increase in mEJP frequency; however, this increase was not significantly different in comparisons to controls (Fig. 4A,D). Thus, FOR does not appear to affect spontaneous neurotransmitter release. At higher external Ca^{2+} concentrations (1 mM Ca^{2+}), the EJP amplitude in *for*^{0} null mutants was significantly larger compared to control and genomic rescue larvae (Fig. 4H,I). However, the effects were more severe at lower Ca^{2+} concentrations (0.5 mM Ca^{2+}), demonstrating a Ca^{2+} dependence of the effects of FOR on evoked neurotransmitter release.

The enhancement of evoked neurotransmitter release in the *for*^{0} null mutant was rescued by presynaptic expression of FOR (Fig. 4E). In contrast, neither postsynaptic (Fig. 4F) nor glial (Fig. 4G) expression of FOR rescued the increased neurotransmitter release seen in the *for*^{0} null mutant. These results demonstrate a presynaptic

Journal of Cell Science (2019) 132, jcs227165. doi:10.1242/jcs.227165

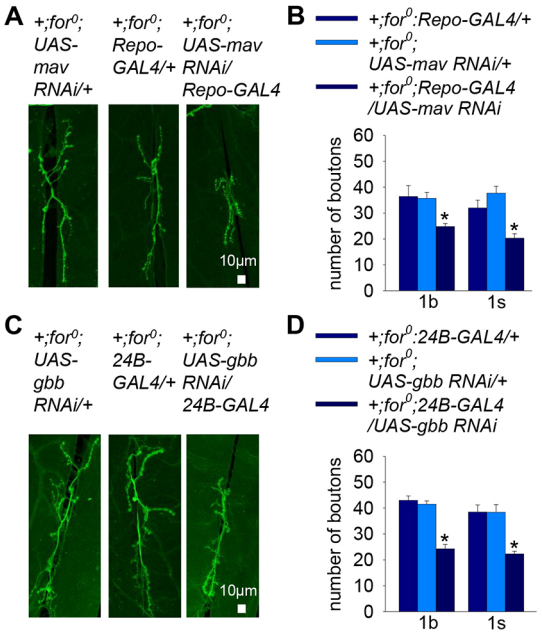

Fig. 3. Glial FOR negatively regulates nerve terminal growth through Mav and Gbb signalling. (A,C) Fixed larval NMJs stained with FITC-conjugated anti-HRP antibody. (B) The increased number of 1b and 1s boutons seen in the *for*^{0} null mutant was rescued by knocking down *mav* in glia (+;*for*^{0};*UAS-mav-RNAi*/*Repo-GAL4*, *n*=6), whereas in *UAS-mav-RNAi* (+;*for*^{0};*UAS-mav-RNAi*/+, *n*=10) or *Repo-GAL4* (+;*for*^{0};*Repo-GAL4*/+, *n*=5) controls, there was no rescue of the increased nerve terminal growth seen in the *for*^{0} null mutants (**P*=0.013 for 1b boutons and **P*=0.003 for 1s boutons). (D) The increased number of 1b and 1s boutons seen in the *for*^{0} null mutant was rescued by knocking down *gbb* in muscle (+;*for*^{0};*UAS-gbb-RNAi*/*24B-GAL4*, *n*=8), whereas in *UAS-gbb-RNAi* (+;*for*^{0};*UAS-gbb-RNAi*/+, *n*=8) or *24B-GAL4* (+;*for*^{0};*24B-GAL4*/+, *n*=4) controls, there was no rescue of the increased nerve terminal growth seen in the *for*^{0} null mutants (**P*<0.001 for 1b and 1s boutons). Values represent the mean±s.e.m. Significance was determined using one-way ANOVA.

role for FOR in neurotransmission. Specifically, presynaptic FOR negatively regulates evoked neurotransmitter release, but does not appear to regulate spontaneous neurotransmitter release.

PKG has been shown to regulate intracellular Ca^{2+} in neuronal and non-neuronal tissues (Ruth et al., 1993; Meriney et al., 1994; Schlossmann et al., 2000). We hypothesized that the increased neurotransmitter release seen in *for*^{0} null mutants in response to low-frequency stimulation may be due to changes in presynaptic Ca^{2+} levels. To test this hypothesis, we assayed presynaptic Ca^{2+} signals evoked by single action potentials at high temporal resolution using Oregon Green 488 BAPTA-1 conjugated to 10-kDa Dextran (OGB-1). This approach is sensitive enough to detect changes in presynaptic Ca^{2+} in response to single pulses (Macleod et al., 2002). Nerve terminals were forward filled with the indicator and a single pulse was delivered to the motor axons. Signals from single type 1b boutons at the ends of nerve branches were analysed. Absolute fluorescence prior to stimulation was not significantly different between genotypes [control, 296.60±35.59 arbitrary units (a.u.); *for*^{0} null, 288.89±28.84 a.u.; genomic rescue, 292.29±80.08 a.u.]. We found that peak amplitudes of Ca^{2+} signals in response to single pulses were significantly enhanced by 40% in the *for*^{0} null mutant compared to the control and the genomic rescue (Fig. 4J,K). This increase was large enough to account for the increased neurotransmitter release seen in *for*^{0} null mutants (see Discussion). Overall, FOR inhibits evoked neurotransmitter release by negatively regulating both nerve terminal growth and presynaptic Ca^{2+} levels during low-frequency stimulation.

Presynaptic FOR is required for SV recycling

We tested the ability of *for*^{0} null mutants to maintain neurotransmitter release during high-frequency stimulation. There were no significant differences in the initial EJP amplitudes between genotypes in saline with 2 mM Ca^{2+} (data not shown). EJP amplitudes in *for*^{0} null mutants displayed a significant decline when stimulated at 10 Hz for 5 min in 2 mM Ca^{2+} in comparison to control and rescue larvae (Fig. 5A,B). We hypothesized that the underlying mechanism for the depression in neurotransmitter release seen in *for*^{0} null mutants during high-frequency stimulation could be a defect in SV recycling. We examined the role of *for* in SV recycling using our mutant and rescue genotypes. To accomplish this, we used the lipophilic styryl dye FM1-43 (Betz and Bewick, 1992) to assess SV cycling, measuring FM1-43 uptake by stimulating preparations with high K^{+} saline for 2 min in the presence of FM1-43. We found a significant impairment in FM1-43 uptake in *for*^{0} null mutants in comparison to control and genomic rescue larvae (Fig. 5C,D). To determine whether this impairment was due to a defect in SV exocytosis, we next measured FM1-43 unloading by applying high K^{+} saline for 2 min and calculating the released fraction. We found that *for*^{0} null mutants released a similar fraction of FM1-43 in comparison to control and genomic rescue lines (Fig. 5C,E), demonstrating that recycled SVs could be released. Consequently, the defects in FM1-43 uptake are likely attributable to an impairment in SV endocytosis.

It is unknown whether presynaptic, postsynaptic or glial PKG regulates SV endocytosis. We used tissue-specific rescues to determine whether FOR was required for SV endocytosis presynaptically, postsynaptically (muscle) or in glia. Presynaptic expression of FOR rescued the reduction in FM1-43 uptake in *for*^{0} null mutant backgrounds (Fig. 5F,G), whereas postsynaptic or glial expression of FOR did not rescue the impaired FM1-43 uptake of *for*^{0} null mutants (Fig. 5I,K). The released fraction was similar between all genotypes (Fig. 5F,H,J,L). From these data, we conclude that presynaptic FOR is required for SV endocytosis.

The effect of FOR on synaptic transmission is distinct from its effect on nerve terminal growth

Effects on synaptic transmission and nerve terminal growth have been shown in some cases to be interrelated (Budnik et al., 1990; Stewart et al., 1996; Davis and Goodman, 1998). However, these processes are not always tightly linked (Romero-Pozuelo et al., 2007, 2014; Dason et al., 2009). We next tested whether the increased neurotransmitter release in the *for*^{0} null mutant (Fig. 4A,B) could occur independently of changes in nerve terminal growth. To separate the effect of FOR on nerve terminal growth from its effect on synaptic transmission, we acutely inactivated FOR using FlAsH-FALI (Marek and Davis, 2002). This technique is based on the use of a tetracysteine epitope tag (4c) that binds to membrane-permeable FlAsH-EDT_2. When excited with light of the appropriate wavelength, FlAsH-EDT_2 bound to the 4c tag inactivates the tagged protein with a half-maximal distance of ∼40 Å through the generation of reactive oxygen species (Beck et al., 2002). FlAsH-FALI has been shown to be very selective in inactivating only the tagged protein. For example, photoinactivation of dynamin or its binding partner EndophilinA results in different endocytic defects, thereby demonstrating the specificity of FlAsH-FALI (Kasprowicz et al., 2014). When we expressed FOR-flag-4c, under the control of endogenous promoters in a *for*^{0} mutant background, we rescued both the increased nerve terminal growth (Fig. 6A,B)

Journal of Cell Science (2019) 132, jcs227165. doi:10.1242/jcs.227165

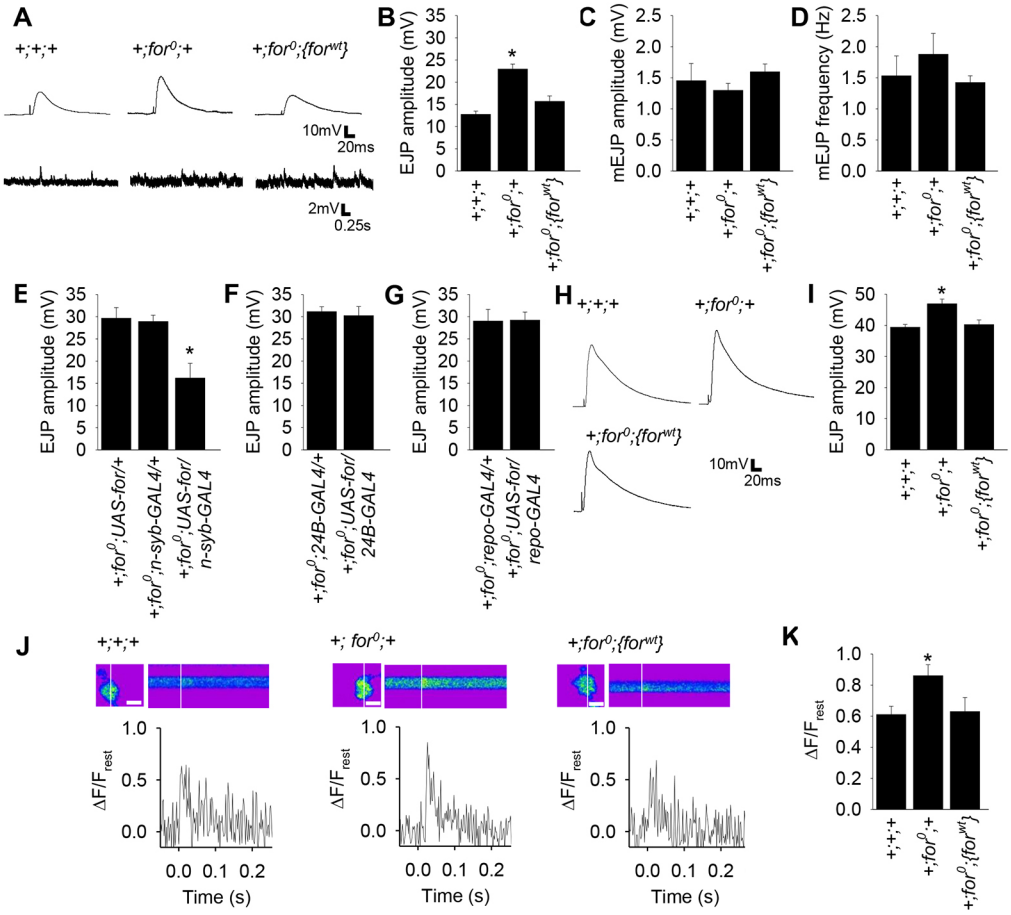

Fig. 4. Presynaptic FOR negatively regulates neurotransmitter release and presynaptic Ca^{2+} in response to low-frequency stimulation. (A) Representative traces of EJPs and mEJPs. Preparations were maintained in HL6 (0.5 mM Ca^{2+}) saline. (B) The amplitude of evoked EJPs from *for*^{0} null mutants (+;*for*^{0};+, *n*=6) was significantly increased (**P*<0.001) in comparison to control (+;+;+, *n*=8) and rescue (+;*for*^{0};{*for*^{wt}}, *n*=8) lines. (C,D) There were no significant differences in mEJP amplitude (*P*=0.481) or frequency (*P*=0.503) between genotypes. (E) The increased evoked EJP amplitudes seen in *for*^{0} null mutants were rescued by neuronal expression of FOR (+;*for*^{0};*UAS-for-flag-4c*/*n-syb-GAL4*, *n*=6), but in *UAS-for* (+;*for*^{0};*UAS-for-flag-4c*/+, *n*=6) or *n-syb-GAL4* (+;*for*^{0};*n-syb-GAL4*/+, *n*=6) controls, there was no rescue of the increased EJP amplitudes seen in *for*^{0} null mutants (**P*=0.002). (F,G) The increased evoked EJP amplitudes seen in *for*^{0} null mutants were not rescued by muscle (*n*=6) or glial (*n*=6) expression of FOR (*P*>0.05). (H) Representative traces of EJPs. Preparations were maintained in HL6 (1 mM Ca^{2+}) saline. (I) The amplitude of evoked EJPs from *for*^{0} null mutants (+;*for*^{0};+, *n*=10) was significantly increased (**P*<0.01) in comparison to control (+;+;+, *n*=8) and rescue (+;*for*^{0};{*for*^{wt}}, *n*=9) lines. (J) Representative images of changes in fluorescence detected by line scanning of Ib boutons loaded with OGB-1. Representative traces of relative fluorescence changes in response to a single stimulus pulse are plotted below each image. Scale bars: 6 µm. (K) There was a significant increase in the peak amplitude of Ca^{2+} signals of the *for*^{0} null mutant (+;*for*^{0};+, *n*=11) in comparison to its control (+;+;+, *n*=16) and genomic rescue (+;*for*^{0};{*for*^{wt}}, *n*=16) genotypes (**P*=0.024). $\Delta F/F_{rest}$ was calculated by dividing the change in fluorescence in response to stimulation (ΔF) by the value of fluorescence at rest (F_{rest}) before nerve stimulation. Values represent the mean±s.e.m. Significance was determined using one-way ANOVA.

and increased synaptic transmission (Fig. 6C,D) previously seen in the *for*^{0} null mutant (Figs 2B and 4B). Thus, FOR-flag-4c recapitulates FOR function for both nerve terminal growth and synaptic transmission. We next investigated whether acute photoinactivation of FOR affected synaptic transmission. We incubated NMJs with FlAsH-EDT_2, then washed unbound FlAsH-EDT_2 and illuminated with epifluorescent light filtered at 488 nm (see Materials and Methods for details). In controls, incubation with FlAsH-EDT_2 and illumination with light had no effect on EJP amplitude (Fig. 6C,D). However, the amplitude of evoked EJPs in response to low-frequency stimulation (0.05 Hz) of larvae expressing FOR-flag-4c in *for*^{0} null mutants was significantly enhanced following light inactivation compared to controls (Fig. 6C,D). The increase in synaptic transmission occurs in a timeframe that is too fast for changes in nerve terminal growth to occur (Ataman et al., 2008). This demonstrates that the effect of FOR on synaptic transmission can occur without its effect on nerve terminal growth.

The effects of FOR on SV exocytosis and endocytosis are distinct

Increased neurotransmitter release can lead to depletion of the readily releasable pool of SVs (Zucker and Regehr, 2002) and this could contribute to the increased depression seen in *for*^{0} null mutants during high-frequency stimulation (Fig. 5A,B). Therefore, we next investigated whether the effect of FOR on SV recycling was separate from its effect on neurotransmitter release. In order to test the function of FOR during endocytosis without affecting FOR during exocytosis, we used a *shi* temperature-sensitive dynamin mutant to deplete the entire SV pool and thereby uncouple exocytosis and endocytosis. Prolonged stimulation of *shi* mutant NMJs at nonpermissive temperature (30°C) blocks SV recycling, which leads to loss of SVs (Macleod et al., 2004; Dason et al., 2010) and neurotransmitter release (Delgado et al., 2000; Dason et al., 2010). This block is reversible and SVs reform when returned to permissive temperatures (22°C). This block does not occur at wild-type NMJs (Dason et al., 2010). We recorded EJPs in response to

Journal of Cell Science (2019) 132, jcs227165. doi:10.1242/jcs.227165

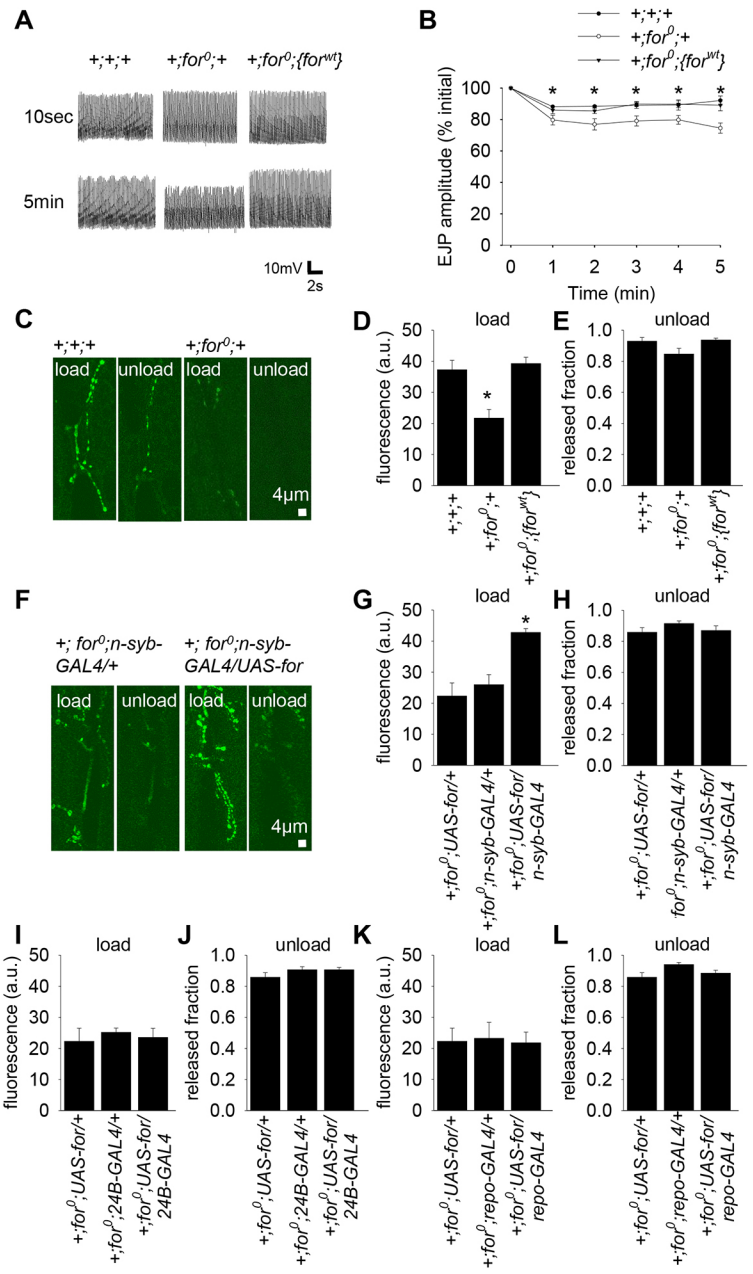

Fig. 5. Presynaptic FOR regulates SV endocytosis. (A) Representative traces of EJPs. (B) The EJP amplitudes in *for*^{0} null mutants (+;*for*^{0};+, *n*=7) were significantly reduced when stimulated at 10 Hz in 2 mM Ca^{2+} in comparison to control (+;+;+, *n*=7) and genomic rescue (+;*for*^{0};{*for*^{wt}}, *n*=7) larvae (**P*<0.05). (C,F) Representative images of presynaptic terminals loaded with FM1-43 during high K^{+} for 2 min and subsequently unloaded with high K^{+} stimulation. Preparations were then washed in 0 mM Ca^{2+} HL6 (with 75 µM Advasep-7 for the first 1 min) for 5 min to remove extracellular FM1-43 and fluorescence was measured. Then, high K^{+} saline was reapplied for 2 min to cause unloading and fluorescence was measured again (unload). (D) *for*^{0} null mutants (*n*=16) took up significantly less FM1-43 than control (*n*=9) and genomic rescue (*n*=10) genotypes (**P*<0.001), demonstrating impaired SV recycling. (E) A similar fraction of FM1-43 was released in all genotypes, demonstrating that recycled SVs could undergo exocytosis (*P*=0.058). (G) This impairment of SV recycling was rescued by neuronal-specific rescue of FOR (+;*for*^{0};*UAS-for-flag-4c*/*n-syb-GAL4*, *n*=6), but in *UAS-for* (+;*for*^{0};*UAS-for-flag-4c*/+, *n*=6) or *n-syb-GAL4* (+;*for*^{0};*n-syb-GAL4*/+, *n*=6) controls, there was no rescue of the impaired SV recycling in *for*^{0} null mutants (**P*<0.001). (I,K) Muscle (*n*=6)- or glial (*n*=6)-specific expression of FOR in *for*^{0} null mutant background controls did not rescue the impaired SV recycling in *for*^{0} null mutants (*P*>0.05). (H,J,L) A similar fraction of FM1-43 was released in all genotypes (*P*>0.05). Fluorescence (F) was reported with background F subtracted. Values represent the mean ±s.e.m. Significance was determined using one-way ANOVA.

0.05 Hz stimulation at 22°C to assess synaptic transmission prior to SV depletion, followed by a stimulus train (10 Hz, 12 min) at 30°C designed to deplete the terminals of SVs. We then assessed recovery of synaptic transmission by recording EJPs in response to 0.05 Hz stimulation at 22°C for the subsequent 20 min (Fig. S4A,B). Consistent with previous studies, we found that synaptic transmission in *shi* mutants was progressively impaired at the restrictive temperature (30°C), but recovered after return to the permissive temperature (Delgado et al., 2000; Dason et al., 2010). When we expressed FOR-flag-4c in a *shi*, *for*^{0} double-mutant background, there was a gradual loss of EJP amplitude during stimulation at the restrictive temperature and recovery of synaptic transmission after return to the permissive temperature (Fig. S4A,B). Recovery of synaptic transmission was similar between *shi* mutants with wild-type FOR and *shi* mutants that expressed FOR-flag-4c in a *for*^{0} mutant background, demonstrating that FOR-flag-4c can recapitulate FOR function during SV recycling.

We then modified our *shi* protocol to use FlAsH-FALI to test the effects of acutely photoinactivating FOR after normal stimulus-dependent exocytosis (Fig. 7A). We recorded EJPs in response to 0.05 Hz stimulation at 22°C to assess synaptic transmission prior to SV depletion, followed by a stimulus train (10 Hz, 12 min) at 30°C designed to deplete the terminals of SVs. We kept both control (*shi;+;+*) and experimental (*shi;for*^{0}*;{for*$^{flag\text{-}4c}$*}*) NMJs at 30°C for an additional 18 min during our FlAsH-FALI protocol (9 min incubation with FlAsH-EDT_2, followed by 4 min wash with BAL buffer to remove unbound FlAsH, and then illumination with epifluorescent light filtered at 488 nm for 5 min to photoinactivate FOR). Recovery of synaptic transmission was then assessed by recording EJPs in response to 0.05 Hz stimulation at 22°C. Recovery of synaptic transmission in control larvae was similar to recovery in the absence of FlAsH-EDT_2 (Fig. 7B,C), whereas acute photoinactivation of FOR resulted in a significant reduction in the recovery of synaptic transmission after return to the permissive

Journal of Cell Science (2019) 132, jcs227165. doi:10.1242/jcs.227165

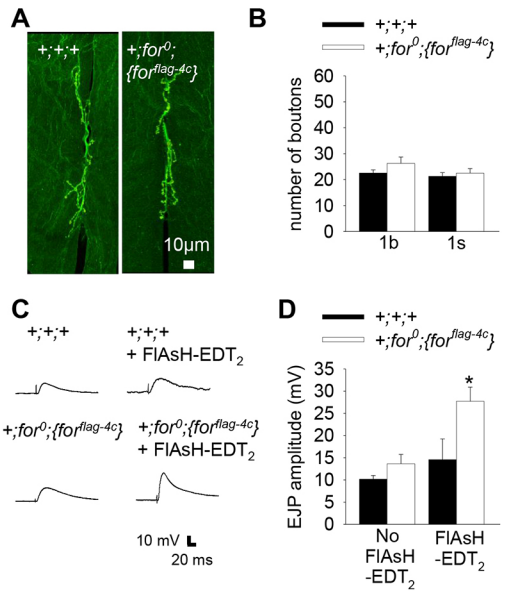

Fig. 6. The effects of FOR on neurotransmitter release can occur independently of changes in nerve terminal growth. (A) Representative images of third-instar larval NMJs stained with anti-HRP. (B) The number of 1b and 1s boutons was not significantly different between rescue (+;for^0;{$for^{flag\text{-}4c}$}, n=6) and control (+;+;+, n=6) genotypes (P>0.05). (C) Representative traces of EJPs. Preparations were maintained in HL6 (0.5 mM Ca^{2+}) saline. (D) There was no difference in the amplitude of evoked EJPs between rescue (+;for^0;{$for^{flag\text{-}4c}$}, n=6) and control (+;+;+, n=6) genotypes in the absence of FlAsH-FALI. Acute photoinactivation of FOR by FlAsH-FALI resulted in a significant increase in the amplitude of evoked EJPs between rescue (+;for^0;{$for^{flag\text{-}4c}$}) and control (+;+;+) genotypes (*P<0.05). Values represent the mean±s.e.m. Significance was determined using unpaired t-tests.

temperature compared to controls (Fig. 7B,C). This demonstrates that acute inactivation of FOR reduces the recovery of synaptic transmission, likely by impairing SV endocytosis.

To determine whether the impairment in recovery of synaptic transmission following the acute inactivation of FOR was due to reduced SV endocytosis, we assessed SV recycling using the lipophilic styryl dye FM4-64 (Fig. 7D). We used FM4-64 because the excitation and emission spectra of FM1-43 overlap with those of FlAsH-EDT_2 more extensively than those of FM4-64. Control (*shi;+;+*) and experimental (*shi;for^0;{for$^{flag\text{-}4c}$}*) NMJs were stimulated with high K^+ saline for 10 min at 30°C to trap SVs, followed by FlAsH-FALI at 30°C (9 min incubation with FlAsH-EDT_2, 4 min wash with BAL buffer to remove unbound FlAsH, and then illumination with epifluorescent light filtered at 488 nm for 5 min to photoinactivate FOR). SV endocytosis was then assayed by incubating preparations with FM4-64 for 20 min at 22°C, followed by a 10-min wash to remove extracellular FM4-64. In the absence of FlAsH-FALI, we found no significant difference in the amount of FM4-64 uptake between control (*shi;+;+*) and experimental (*shi;for^0;for$^{flag\text{-}4c}$*) NMJs (Fig. S4C,D). FM4-64 uptake in control NMJs subjected to the FlAsH-FALI protocol was similar to FM4-64 uptake in the absence of FlAsH-EDT_2 (Fig. 7E,F). In contrast, acute photoinactivation of FOR resulted in a significant reduction in FM4-64 uptake (Fig. 7E,F). The released fraction of FM4-64 following high K^+ stimulation was similar for all genotypes (Fig. 7G; Fig. S4E), demonstrating that recycled SVs could be released. Overall, the FM4-64 data are consistent with our electrophysiology data and clearly demonstrate that acute inactivation of FOR, following normal-stimulus dependent exocytosis, results in impaired recovery of synaptic transmission due to reduced SV endocytosis.

DISCUSSION

Our study is the first to experimentally separate the exocytic and endocytic functions of a PKG in neurotransmission. We show that, during periods of low synaptic activity, presynaptic FOR negatively regulates neurotransmitter release by inhibiting presynaptic Ca^{2+} levels. During periods of high synaptic activity, presynaptic FOR maintains neurotransmission by facilitating SV recycling. In addition, we show that glial FOR negatively regulates nerve terminal growth through Mav and Gbb signalling, and this effect is likely distinct from its effects on neurotransmitter release and SV recycling.

Glial FOR negatively regulates nerve terminal growth through Mav and Gbb signalling

We found that *for^0* null mutants have increased nerve terminal growth. PKG has previously been shown to regulate axon guidance and synaptogenesis (Peng et al., 2016; Sild et al., 2016). Expression of a dominant-negative form of PKG in *Xenopus* radial glia impairs glial motility and synaptogenesis (Sild et al., 2016). Here, we show that glial FOR negatively regulates nerve terminal growth, whereas presynaptic and postsynaptic FOR do not regulate nerve terminal growth. *Drosophila* glia regulate nerve terminal growth by releasing the TGF-β ligand, Mav, to modulate TGF-β/BMP retrograde signalling, which leads to the addition of new synaptic boutons (Fuentes-Medel et al., 2012). Glial Mav regulates nerve terminal growth through muscle-derived Gbb, the *Drosophila* TGF-β/BMP homologue (Fuentes-Medel et al., 2012). We found that glial-specific knockdown of Mav or muscle-specific knockdown of Gbb rescues the nerve terminal overgrowth phenotype of *for^0* null mutants. This suggests that FOR acts through Mav and Gbb to negatively regulate nerve terminal growth, although it remains possible that FOR functions in a parallel pathway to Mav and Gbb. Interestingly, FOR also regulates TGF-β/BMP signalling in the developing wing of *Drosophila* (Schleede and Blair, 2015). PKG regulates intracellular Ca^{2+} levels in rat glial cell cultures (Willmott et al., 2000). Thus, it is tempting to speculate that FOR can affect Mav secretion by regulating Ca^{2+} levels in glia. However, currently, little is known about the mechanisms underlying Mav secretion from glia.

The effects of FOR on synaptic transmission are dependent on the type of synaptic activity

PKG has been implicated in regulating neurotransmitter release (Yawo, 1999; Wei et al., 2002; Luo et al., 2012). However, these studies have been contradictory, suggesting both a stimulatory and inhibitory role. Reconciling these findings, we show that FOR plays an inhibitory role in neurotransmitter release during low-frequency stimulation and a facilitatory role in SV recycling that can maintain sustained neurotransmitter release during high-frequency stimulation. Interestingly, the frequency of spontaneous neurotransmitter release is not altered in *for^0* null mutants (Fig. 4D), despite *for^0* null mutants having more synaptic boutons, and thus more active zones, per NMJ. Release probability for evoked and spontaneous neurotransmitter release at individual active zones at the *Drosophila* larval NMJ are not correlated, suggesting that they are independently regulated (Melom et al., 2013). Thus, FOR may be having a selective effect on active zones involved in evoked neurotransmitter release. Alternatively, some kind of homeostasis (Stewart et al., 1996; Davis and Goodman, 1998) may be occurring in the *for^0* null mutant to compensate for the increased nerve terminal growth.

Journal of Cell Science (2019) 132, jcs227165. doi:10.1242/jcs.227165

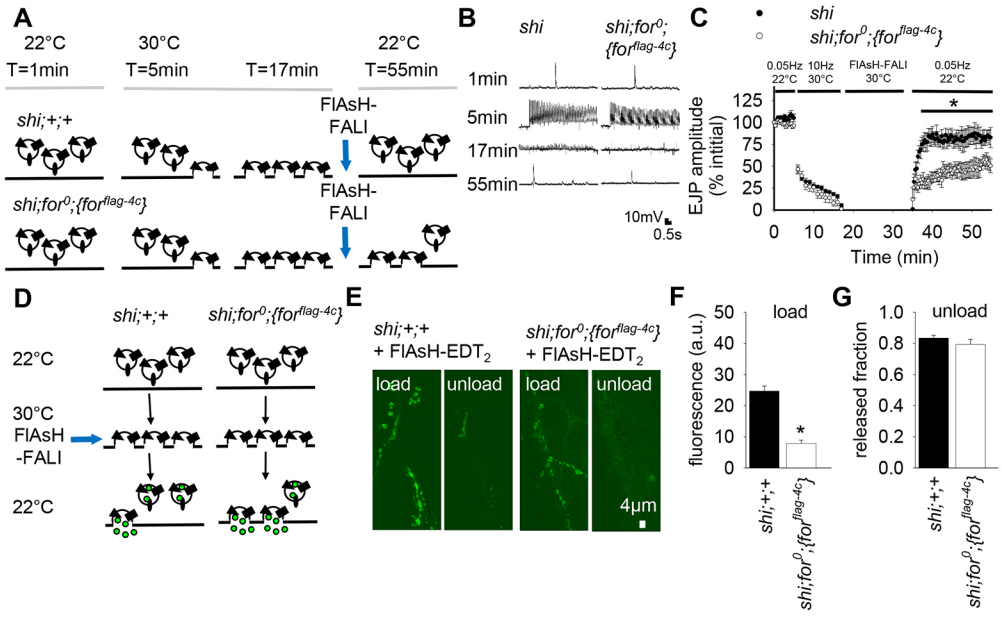

Fig. 7. Acute inactivation of FOR, following normal stimulus-dependent SV exocytosis, impairs SV endocytosis. (A) Schematic of the electrophysiology experimental protocol. (B) Representative traces of EJPs. *shi* preparations were maintained in HL6 (1 mM Ca^{2+}) saline. The segmental nerve was stimulated at 0.05 Hz for 5 min at 22°C, followed by 10 Hz stimulation for 12 min at 30°C, and then FlAsH-FALI at 30°C (9 min incubation with FlAsH-EDT_2, 4 min wash with BAL buffer to remove unbound FlAsH, and then illumination with epifluorescent light filtered at 488 nm for 5 min to photoinactivate FOR). Next, recovery of synaptic transmission was assessed by stimulating the segmental nerve at 0.05 Hz for 20 min at 22°C. (C) Recovery of synaptic transmission was significantly reduced following FOR photoinactivation (*P<0.05; n=7). (D) Schematic of the FM4-64 experimental protocol. (E) Representative images. Preparations were stimulated (90 mM K^+ for 10 min) at 30°C, followed by FlAsH-FALI at 30°C (9 min incubation with FlAsH-EDT_2, 4 min wash with BAL buffer to remove unbound FlAsH, and then illumination with epifluorescent light filtered at 488 nm for 5 min to photoinactivate FOR). Endocytosis was assayed by incubating preparations with 10 µM FM4-64 for 20 min at 22°C (load), then washing in 0 mM Ca^{2+} HL6 (with 75 µM Advasep-7 for the first 2 min) for 10 min to remove extracellular FM4-64 and fluorescence (F) was then measured. 90 mM K^+ saline was reapplied for 10 min to cause unloading and F measured again (unload). (F) Inactivation of FOR significantly reduced FM4-64 loading (*P<0.0001; n=6). (G) A similar fraction of FM4-64 was released, demonstrating that recycled SVs could undergo exocytosis (P=0.2828; n=6). Values represent the mean±s.e.m. Significance was determined using unpaired *t*-tests.

FOR negatively regulates neurotransmitter release and presynaptic Ca^{2+} levels in response to low-frequency stimulation

The increased neurotransmitter release seen in the *for*^{0} null mutant is likely due to both increased nerve terminal growth and increased presynaptic Ca^{2+} entry. PKG has been reported to affect Ca^{2+} levels and currents in several tissues (Ruth et al., 1993; Meriney et al., 1994; Schlossmann et al., 2000). However, studies examining the effects of PKG on neurotransmitter release did not correlate these changes with changes in presynaptic Ca^{2+} signals (Gray et al., 1999; Yawo, 1999; Luo et al., 2012). We found that the *for*^{0} null mutant had significantly increased presynaptic Ca^{2+} signals evoked by single action potentials. Neurotransmitter release varies as a fourth-order function of Ca^{2+} (Dodge and Rahamimoff, 1967; Augustine and Charlton, 1986). Assuming a fourth-power relationship, the increased amplitude of Ca^{2+} signals observed in the absence of FOR was sufficient to account for the twofold increase in neurotransmitter release.

The most plausible mechanistic explanations for the increased presynaptic Ca^{2+} levels are direct or indirect regulation of Ca^{2+} channels by FOR. A recent study reported that PKG downregulates L-type Ca^{2+} channel activity in HEK-293 cells through phosphorylation of two serine residues in the intracellular loop of the pore-forming $Ca_v\alpha1$ subunit (Sandoval et al., 2017). Ca^{2+} channels found in presynaptic boutons at the *Drosophila* larval NMJ are likely N- or P/Q-type (Rieckhof et al., 2003; Macleod et al., 2006). PKG agonists inhibit N-type Ca^{2+} channel currents in dorsal root ganglion neurons (Yoshimura et al., 2001); thus, it remains possible that a similar type of regulation by PKG occurs for N- or P/Q-type channels. Alternatively, the effects of FOR on presynaptic Ca^{2+} could be a consequence of the modulation of K^+ channels. PKG phosphorylates Ca^{2+}-activated K^+ channels (Alioua et al., 1998; Fukao et al., 1999; Zhou et al., 2001; Ferreira et al., 2015) and PKG inhibitors reduce Ca^{2+}-activated K^+ channel activity (Klyachko et al., 2001). Interestingly, cultured *Drosophila* neurons of an allelic variant of *for* with higher PKG activity displayed increased voltage-dependent K^+ currents (Renger et al., 1999). A reduction in K^+ currents in *for*^{0} null mutants could increase action potential duration, leading to increased presynaptic Ca^{2+} entry and increased neurotransmitter release.

FOR maintains sustained synaptic transmission during high-frequency stimulation by facilitating SV endocytosis

Neurotransmitter release was significantly reduced in *for*^{0} null mutants during high-frequency stimulation (Fig. 5B). The inability of *for*^{0} null mutants to maintain normal levels of neurotransmitter release during high-frequency stimulation is mechanistically consistent with a defect in SV recycling. Pharmacological inhibition (Petrov et al., 2008; Eguchi et al., 2012; Taoufiq et al., 2013) and RNA interference (RNAi) knockdown of PKG (Collado-Alsina et al., 2014) reduces SV endocytosis. However, these studies did not experimentally separate exocytic and endocytic functions of PKG. Here, we used FlAsH-FALI in conjunction with a temperature-sensitive *shi* mutant to tease apart the role of FOR in SV exocytosis and endocytosis by dissociating these two processes. We used FlAsH-FALI to photoinactivate FOR following SV exocytosis but prior to SV endocytosis, and then assayed SV recycling using electrophysiology and FM4-64 imaging. We depleted the entire pool

Journal of Cell Science (2019) 132, jcs227165. doi:10.1242/jcs.227165

of SVs and then tested the role of FOR in SV endocytosis. By temporally uncoupling SV exocytosis and endocytosis, and then acutely inactivating FOR, we show that FOR is necessary for efficient endocytosis of SVs that have undergone exocytosis using a functional FOR protein. This approach can be modified to study the exocytic and endocytic functions of other kinases in mammalian preparations by using FALI in conjunction with dynamin inhibitors, such as dynasore (Macia et al., 2006). In addition, we found that presynaptic, but not postsynaptic or glial, FOR was required for SV recycling. Contributions of presynaptic, postsynaptic and glial PKG were not addressed in previous studies. PKG is thought to function at a step between the upregulation of cGMP and phosphatidylinositol 4,5-bisphosphate (PIP_2) levels through a Rho kinase (Taoufiq et al., 2013). Thus, the effects of FOR on SV endocytosis may be through PIP_2 signalling and the recruitment of AP-2 and Clathrin proteins to sites of endocytosis.

Kinases have multiple functions and are often thought of as pleiotropic. Kinases can phosphorylate multiple targets, be expressed in different cells, have different subcellular expression patterns and be temporally activated at different times, all of which are means of pleiotropy. FOR has been implicated in behavioural pleiotropy (Allen et al., 2017; Anreiter et al., 2017; Allen et al., 2018; Anreiter and Sokolowski, 2018). Here, we show distinct spatial and temporal requirements for FOR at the synapse. Glial FOR is required for the developmental effects of FOR on nerve terminal growth, whereas presynaptic FOR is required for the acute effects of FOR on neurotransmitter release and SV recycling. Thus, the developmental effects of FOR are likely independent from its effects on SV exocytosis and endocytosis. Furthermore, we show that the effects of FOR on neurotransmitter release and SV recycling can be temporally separated. We conclude that FOR plays critical and distinct roles in regulating nerve terminal growth and coupling SV exocytosis and endocytosis. Our work highlights the multifaceted nature of kinases and demonstrates the importance of temporally and spatially targeting them when studying their functions.

MATERIALS AND METHODS

Fly stocks

Fly stocks were grown in uncrowded conditions at 25°C on molasses-based fly medium (Anreiter et al., 2016). Mid-third-instar larvae were used for all experiments. A *sitter* strain (+;+;+) was used as a wild-type control and all lines were backcrossed to it (Allen et al., 2017). The for^{0} null mutant contains a 35 kb deletion that removes the entire *for* locus (Allen et al., 2017). $\{for^{wt}\}$ is a genomic rescue inserted on the third chromosome that contains a BAC with the entire *for* locus (Allen et al., 2017). $\{for^{flag\text{-}4c}\}$ is a genomic rescue generated in this study that contains a BAC with the entire *for* locus with a flag tag and a tetracysteine (4c) tag on the C-terminus. The GAL4/UAS system (Brand and Perrimon, 1993) was used for tissue-specific expression of transgenes. *n-syb-GAL4* was used to drive expression in neurons (Verstreken et al., 2009). *24B-GAL4* was used to drive expression in muscles (Sweeney et al., 1995). *Repo-GAL4* or *46F-GAL4* was used to drive expression in glia (Sepp et al., 2001; Brink et al., 2012). *da-GAL4* was used as a ubiquitous driver (Wodarz et al., 1995). for^{pr3}*-GAL4* was used to drive expression of *UAS-mCD8-GFP* in a subset of cells that express *for* (Allen et al., 2018). *UAS-mav-RNAi* was used to knock down *mav* (Fuentes-Medel et al., 2012). *UAS-gbb-RNAi* was used to knock down *gbb* (Tian and Jiang, 2014). *UAS-for-flag-4c* was generated in this study and used to express FOR with a flag-4c tag on the C-terminus in selective tissues. The temperature-sensitive *shi* mutant (Grigliatti et al., 1973) was used to reversibly block SV recycling.

Recombineering

Recombineering-mediated tagging was performed as previously described (Venken et al., 2008). A modified P(acman) vector containing a full-length 35 kb genomic fragment of the *for* gene was used (Allen et al., 2017). A PCR fragment coding for flag and a tetracysteine cassette (4c) was amplified from a PL-452 C-flag-4c plasmid (Addgene plasmid #19180; Venken et al., 2008) using the forward primer 5′-ATACAACAAACTTTGATGACTATCCTCCCGATCCTGAGGGTCCGCCGCCAGATGATGTCACTGGATGGGACAAGGACTTCGGTCCCTCGAGGGGATCCATGG-3′ and the reverse primer 5′-TGGCTTTCATATCCTCCTGGTTTTCTGCAGCAGAAGCGTTTAGAGAGCATCGTCTAGGAAACGGGTTCTGATTCTCCTCATTAGGGCTCCATGCAGCAG-3′. The fragment was inserted onto the C-terminal end of *for* using recombineering (Venken et al., 2008) and a galk selection method (Warming et al., 2005). The BAC was incorporated into the fly's genome using ϕC31 integration into the attP2 landing site on the third chromosome. Transgenesis was performed by BestGene Inc. (Chino Hills, CA).

Cloning

The open reading frame (ORF) of *for* P1 was amplified from a pUASTattB-P1 vector with the forward primer 5′-GCGGCCGCATGCGTTTCTGCTTTGATCG-3′ and the reverse primer 5′-CCATGGATCCCCTCGAGGGACCGAAGTCCTTGTCCCATCCAGTGAC-3′. A PCR fragment coding for flag and a tetracysteine cassette (4c) was amplified from a PL-452 C-flag-4c plasmid (Addgene plasmid #19180; Venken et al., 2008) using the forward primer 5′-GGTCCCTCGAGGGGATCCATGG-3′ and the reverse primer 5′- TATGCGGCCGCTTAGGGCTCCATGCAG-CAG-3′. A fusion PCR protocol was used to generate a *for*-flag-4c construct (Hobert, 2002). *for*-flag-4c was then cloned into the pUASTattB vector (Bischof et al., 2007). The pUASTattB vector was incorporated into the fly's genome using ϕC31 integration into the attP2 landing site on the third chromosome. Transgenesis was performed by BestGene Inc. (Chino Hills, CA).

Western blots

Western blots were performed as previously described (Allen et al., 2017). Briefly, samples were resolved by SDS-PAGE and blots were incubated with a guinea pig polyclonal anti-FOR antibody (1:5000) (Belay et al., 2007) or a mouse monoclonal anti-actin antibody (MAB1501, Sigma-Aldrich; 1:20,000) for 1 h at room temperature. The following day, the membrane was washed, incubated with the secondary antibody for 1 h at room temperature, washed again, and immunoreactivity was then detected using GE Healthcare Amersham ECL Prime Detection Reagent.

Immunohistochemistry

Immunohistochemistry was performed as previously described (Dason et al., 2014). Briefly, fixed preparations were incubated overnight at 4°C with fluorescein isothiocyanate (FITC)-conjugated anti-HRP (1:800; Jackson ImmunoResearch, USA) to visualize neurons, mouse monoclonal anti-BRP (1:100; Developmental Studies Hybridoma Bank, Iowa City, IA; Wagh et al., 2006) to visualize active zones, rabbit anti-Cpx (Huntwork and Littleton, 2007), mouse anti-Gli (Schulte et al., 2003), polyclonal rabbit anti-DSYT2 (also known as Syt1) (1:800; Littleton et al., 1993), mouse monoclonal anti-GFP (1:500; 3E6, Thermo Fisher Scientific), chicken monoclonal anti-GFP (1:500; AA10262, Thermo Fisher Scientific) or mouse monoclonal anti-Flag M2 (1:500; F1804, Sigma-Aldrich; Hampel et al., 2011). All primary antibodies were diluted in blocking solution. Preparations were mounted in Permafluor (Immunon, Pittsburgh, PA) on a glass slide with a cover slip and viewed under a TCS SP5 confocal laser-scanning microscope (Leica, Heidelberg, Germany) with a 63× oil-immersion objective (1.4 NA).

Physiological solutions

All electrophysiological and imaging experiments were conducted in the haemolymph-like solution HL6 (Macleod et al., 2002). $CaCl_2$ concentrations are indicated for each experiment.

Electrophysiology

Intracellular recordings were performed as previously described (Dason et al., 2009). Briefly, the ventral longitudinal muscle fibre 6 (abdominal segment 3) of dissected larvae was impaled with a sharp glass electrode

filled with 3 M KCl (~40 MΩ) to measure spontaneously occurring mEJPs and stimulus-evoked EJPs. All preparations tested had a resting membrane potential of −60 mV to −65 mV. Cut segmental nerves were stimulated at either 0.05 Hz or 10 Hz using a suction electrode. Electrical signals were recorded using the MacLab/4S data acquisition system (ADInstruments).

Ca^{2+} imaging

Motor neurons were forward filled with the Ca^{2+} indicator OGB-1 as previously described (Macleod et al., 2002). The relatively fast Ca^{2+}-binding and -unbinding kinetics of OGB-1 allowed us to measure Ca^{2+} signals in response to single pulses. All experiments with OGB-1 were performed on a Leica TCS SP5 confocal laser-scanning microscope with a 63× water-dipping objective (0.9 NA). Cut segmental nerves were stimulated with single pulses using a suction electrode. A line-scanning method (4 ms per scan) was used to follow Ca^{2+} responses to single pulses in a single 1b bouton with high temporal resolution. Fluorescence (F) was reported using the equation $\Delta F/F_{rest}=(F_{stim}- F_{rest})/F_{rest}$.

FM1-43 imaging

FM1-43 experiments were performed using a Leica TCS SP5 confocal laser-scanning microscope with a 63× water-dipping objective (0.9 NA) as previously described (Dason et al., 2010). Briefly, FM1-43 loading and unloading was induced by high K^+ depolarization using the following high K^+ saline: 25 mM NaCl, 90 mM KCl, 10 mM $NaHCO_3$, 5 mM HEPES, 30 mM sucrose, 5 mM trehalose, 10 mM $MgCl_2$, 2 mM $CaCl_2$, pH 7.2 (Verstreken et al., 2008). Preparations were loaded with FM1-43 (Invitrogen) by high K^+ depolarization for 2 min. Preparations were extensively washed for 5 min in Ca^{2+}-free HL6. To reduce background fluorescence from extracellular FM1-43, 75 µM Advasep-7 was included for the first 1 min of the wash (Kay et al., 1999). After an image of FM1-43 uptake was taken, high K^+ depolarization for 2 min was used to induce exocytosis. Another image was then taken to document FM1-43 unloading. Fluorescence was measured and averaged from three 1b boutons per image. The released fraction was calculated using the following formula: (fluorescence of load–fluorescence of unload)/fluorescence of load.

FM4-64 imaging

FM4-64 experiments were performed using a Leica TCS SP5 confocal laser-scanning microscope with a 63× water-dipping objective (0.9 NA) as previously described (Dason et al., 2010). Briefly, preparations were stimulated with the following high K^+ saline at 30°C to trap SVs: 25 mM NaCl, 90 mM KCl, 10 mM $NaHCO_3$, 5 mM HEPES, 30 mM sucrose, 5 mM trehalose, 10 mM $MgCl_2$, 2 mM $CaCl_2$, pH 7.2 (Verstreken et al., 2008). Preparations were then loaded with 10µM FM4-64 (Invitrogen) for 20 min at 22°C. Preparations were extensively washed for 10 min in Ca^{2+}-free HL6. To reduce background fluorescence from extracellular FM4-64, 75 µM Advasep-7 was included for the first 2 min of the wash (Kay et al., 1999). After an image of FM4-64 uptake was taken, high K^+ depolarization for 10 min was used to induce exocytosis. Another image was then taken to document FM4-64 unloading. The released fraction was calculated using the following formula: (fluorescence of load–fluorescence of unload)/fluorescence of load.

FlAsH-FALI

FlAsH-FALI experiments were performed as previously described (Habets and Verstreken, 2011) using a TC-FlAsH™ II In-Cell Tetracysteine Tag Detection Kit (Green Fluorescence; Thermo Fisher Scientific). Briefly, dissected third-instar larvae were incubated with 1 µM FlAsH-EDT_2 in HL6 for 9 min and then washed with BAL buffer for 4 min to remove unbound FlAsH. Muscle fibres 6 and 7 were illuminated with epifluorescent light filtered at 488 nm for 5 min to photoinactivate FOR.

Statistical analysis

SigmaPlot (version 11.0; Systat Software) was used for statistical analysis. Sample sizes were chosen based on what is appropriate and accepted in this field of research. Unpaired *t*-tests were used for comparing datasets of two groups and one-way ANOVA tests (with a Holm–Sidak post hoc test) were used for comparing datasets of more than two groups. Error bars in all figures represent ±s.e.m.

Acknowledgements

We thank Drs Vanessa Auld, Vivian Budnik and Troy Littleton for fly stocks and antibodies, and Drs Harold Atwood, Joel Levine and Ina Anreiter for comments on an early draft of the manuscript.

Competing interests

The authors declare no competing or financial interests.

Author contributions

Conceptualization: J.S.D., M.B.S.; Methodology: J.S.D.; Validation: J.S.D.; Formal analysis: J.S.D., O.E.V.; Investigation: J.S.D., O.E.V.; Resources: A.M.A., M.B.S.; Writing - original draft: J.S.D.; Writing - review & editing: J.S.D., A.M.A., O.E.V., M.B.S.; Visualization: J.S.D.; Supervision: M.B.S.; Project administration: J.S.D., M.B.S.; Funding acquisition: J.S.D., M.B.S.

Funding

This work was supported by the Natural Sciences and Engineering Research Council of Canada [RGPIN 3397-11 and RGPIN-2016-06185 to M.B.S.; RGPIN 06582 to J.S.D.] and the Heart and Stroke Foundation of Canada [Postdoctoral Fellowship to J.S.D.].

Supplementary information

Supplementary information available online at
http://jcs.biologists.org/lookup/doi/10.1242/jcs.227165.supplemental.

References

Alioua, A., Tanaka, Y., Wallner, M., Hofmann, F., Ruth, P., Meera, P. and Toro, L. (1998). The large conductance, voltage-dependent, and calcium-sensitive K+ channel, Hslo, is a target of cGMP-dependent protein kinase phosphorylation in vivo. *J. Biol. Chem.* **273**, 32950-32956.

Allen, A. M., Anreiter, I., Neville, M. C. and Sokolowski, M. B. (2017). Feeding-related traits are affected by dosage of the *foraging* gene in *Drosophila melanogaster*. *Genetics* **205**, 761-773.

Allen, A. M., Anreiter, I., Vesterberg, A., Douglas, S. J. and Sokolowski, M. B. (2018). Pleiotropy of the *Drosophila melanogaster foraging* gene on larval feeding-related traits. *J. Neurogenet.* **32**, 256-266.

Anreiter, I. and Sokolowski, M. B. (2018). Deciphering pleiotropy: how complex genes regulate behavior. *Commun. Integr. Biol.* **11**, e1447743.

Anreiter, I., Vasquez, O. E., Allen, A. M. and Sokolowski, M. B. (2016). Foraging path-length protocol for *Drosophila melanogaster* larvae. *J Vis Exp.* e53980.

Anreiter, I., Kramer, J. M. and Sokolowski, M. B. (2017). Epigenetic mechanisms modulate differences in *Drosophila foraging* behavior. *Proc. Natl. Acad. Sci. USA* **114**, 12518-12523.

Ataman, B., Ashley, J., Gorczyca, M., Ramachandran, P., Fouquet, W., Sigrist, S. J. and Budnik, V. (2008). Rapid activity-dependent modifications in synaptic structure and function require bidirectional Wnt signaling. *Neuron* **57**, 705-718.

Augustine, G. J. and Charlton, M. P. (1986). Calcium dependence of presynaptic calcium current and post-synaptic response at the squid giant synapse. *J. Physiol.* **381**, 619-640.

Beck, S., Sakurai, T., Eustace, B. K., Beste, G., Schier, R., Rudert, F. and Jay, D. G. (2002). Fluorophore-assisted light inactivation: A high-throughput tool for direct target validation of proteins. *Proteomics* **2**, 247-255.

Belay, A. T., Scheiner, R., So, A. K., Douglas, S. J., Chakaborty-Chatterjee, M., Levine, J. D. and Sokolowski, M. B. (2007). The *foraging* gene of *Drosophila melanogaster*: spatial-expression analysis and sucrose responsiveness. *J. Comp. Neurol.* **504**, 570-582.

Betz, W. J. and Bewick, G. S. (1992). Optical analysis of synaptic vesicle recycling at the frog neuromuscular junction. *Science* **255**, 200-203.

Bischof, J., Maeda, R. K., Hediger, M., Karch, F. and Basler, K. (2007). An optimized transgenesis system for *Drosophila* using germ-line-specific phiC31 integrases. *Proc. Natl. Acad. Sci. USA* **104**, 3312-3317.

Brand, A. H. and Perrimon, N. (1993). Targeted gene expression as a means of altering cell fates and generating dominant phenotypes. *Development* **118**, 401-415.

Brink, D. L., Gilbert, M., Xie, X., Petley-Ragan, L. and Auld, V. J. (2012). Glial processes at the *Drosophila* larval neuromuscular junction match synaptic growth. *PLoS ONE* **7**, e37876.

Budnik, V., Zhong, Y. and Wu, C. F. (1990). Morphological plasticity of motor axons in *Drosophila* mutants with altered excitability. *J. Neurosci.* **10**, 3754-3768.

Cantarutti, K. C., Burgess, J., Brill, J. A. and Dason, J. S. (2018). Type II phosphatidylinositol 4-kinase regulates nerve terminal growth and synaptic vesicle recycling. *J. Neurogenet.* **32**, 230-235.

Chen, C. K., Bregere, C., Paluch, J., Lu, J. F., Dickman, D. K. and Chang, K. T. (2014). Activity-dependent facilitation of Synaptojanin and synaptic vesicle recycling by the Minibrain kinase. *Nat. Commun.* **5**, 4246.

Cho, R. W., Buhl, L. K., Volfson, D., Tran, A., Li, F., Akbergenova, Y. and Littleton, J. T. (2015). Phosphorylation of complexin by PKA regulates activity-dependent spontaneous neurotransmitter release and structural synaptic plasticity. *Neuron* **88**, 749-761.

Clayton, E. L., Evans, G. J. and Cousin, M. A. (2007). Activity-dependent control of bulk endocytosis by protein dephosphorylation in central nerve terminals. *J. Physiol.* **585**, 687-691.

Clayton, E. L., Anggono, V., Smillie, K. J., Chau, N., Robinson, P. J. and Cousin, M. A. (2009). The phospho-dependent dynamin-syndapin interaction triggers activity-dependent bulk endocytosis of synaptic vesicles. *J. Neurosci.* **29**, 7706-7717.

Collado-Alsina, A., Ramírez-Franco, J., Sánchez-Prieto, J. and Torres, M. (2014). The regulation of synaptic vesicle recycling by cGMP-dependent protein kinase type II in cerebellar granule cells under strong and sustained stimulation. *J. Neurosci.* **34**, 8788-8799.

Dason, J. S., Romero-Pozuelo, J., Marin, L., Iyengar, B. G., Klose, M. K., Ferrús, A. and Atwood, H. L. (2009). Frequenin/NCS-1 and the Ca^{2+} channel α_1-subunit co-regulate synaptic transmission and nerve terminal growth. *J. Cell Sci.*. **122**, 4109-4121.

Dason, J. S., Smith, A. J., Marin, L. and Charlton, M. P. (2010). Vesicular sterols are essential for synaptic vesicle cycling. *J. Neurosci.* **30**, 15856-15865.

Dason, J. S., Smith, A. J., Marin, L. and Charlton, M. P. (2014). Cholesterol and F-actin are required for clustering of recycling synaptic vesicle proteins in the presynaptic plasma membrane. *J. Physiol.* **592**, 621-633.

Davis, G. W. and Goodman, C. S. (1998). Synapse-specific control of synaptic efficacy at the terminals of a single neuron. *Nature* **392**, 82-86.

Deák, F., Schoch, S., Liu, X., Südhof, T. C. and Kavalali, E. T. (2004). Synaptobrevin is essential for fast synaptic-vesicle endocytosis. *Nat. Cell Biol.* **6**, 1102-1108.

Delgado, R., Maureira, C., Oliva, C., Kidokoro, Y. and Labarca, P. (2000). Size of vesicle pools, rates of mobilization, and recycling at neuromuscular synapses of a *Drosophila* mutant, *shibire*. *Neuron* **28**, 941-953.

Dodge, F. A. and Rahamimoff, R. (1967). Co-operative action a calcium ions in transmitter release at the neuromuscular junction. *J. Physiol.* **193**, 419-432.

Eguchi, K., Nakanishi, S., Takagi, H., Taoufiq, Z. and Takahashi, T. (2012). Maturation of a PKG-dependent retrograde mechanism for exoendocytic coupling of synaptic vesicles. *Neuron* **74**, 517-529.

Ferreira, R., Wong, R. and Schlichter, L. C. (2015). KCa3.1/IK1 channel regulation by cGMP-dependent protein kinase (PKG) via reactive oxygen species and CaMKII in microglia: An immune modulating feedback system? *Front. Immunol.* **6**, 153.

Fuentes-Medel, Y., Ashley, J., Barria, R., Maloney, R., Freeman, M. and Budnik, V. (2012). Integration of a retrograde signal during synapse formation by glia-secreted TGF-β ligand. *Curr. Biol.* **22**, 1831-1838.

Fukao, M., Mason, H. S., Britton, F. C., Kenyon, J. L., Horowitz, B. and Keef, K. D. (1999). Cyclic GMP-dependent protein kinase activates cloned BKCa channels expressed in mammalian cells by direct phosphorylation at serine 1072. *J. Biol. Chem.* **274**, 10927-10935.

Geng, J., Wang, L., Lee, J. Y., Chen, C.-K. and Chang, K. T. (2016). Phosphorylation of synaptojanin differentially regulates endocytosis of functionally distinct synaptic vesicle pools. *J. Neurosci.* **36**, 8882-8894.

Gray, D. B., Polo-Parada, L., Pilar, G. R., Eang, P., Metzger, R. R., Klann, E. and Meriney, S. D. (1999). A nitric oxide/cyclic GMP-dependent protein kinase pathway alters transmitter release and inhibition by somatostatin at a site downstream of calcium entry. *J. Neurochem.* **72**, 1981-1990.

Grigliatti, T. A., Hall, L., Rosenbluth, R. and Suzuki, D. T. (1973). Temperature-sensitive mutations in *Drosophila melanogaster*. XIV. A selection of immobile adults. *Mol. Gen. Genet.* **120**, 104-114.

Habets, R. L. and Verstreken, P. (2011). FlAsH-FALI inactivation of a protein at the third-instar neuromuscular junction. *Cold Spring Harb. Protoc.* **2011**, pdb.prot5597.

Hampel, S., Chung, P., McKellar, C. E., Hall, D., Looger, L. L. and Simpson, J. H. (2011). Drosophila Brainbow: a recombinase-based fluorescence labeling technique to subdivide neural expression patterns. *Nat. Methods* **8**, 253-259.

Harris, K. P. and Littleton, J. T. (2015). Transmission, Development, and Plasticity of Synapses. *Genetics* **201**, 345-375.

Haucke, V., Neher, E. and Sigrist, S. J. (2011). Protein scaffolds in the coupling of synaptic exocytosis and endocytosis. *Nat. Rev. Neurosci.* **12**, 127-138.

Heerssen, H., Fetter, R. D. and Davis, G. W. (2008). Clathrin dependence of synaptic-vesicle formation at the Drosophila neuromuscular junction. *Curr. Biol.* **18**, 401-409.

Hobert, O. (2002). PCR fusion-based approach to create reporter gene constructs for expression analysis in transgenic *C. elegans*. *BioTechniques* **32**, 728-730.

Hosoi, N., Holt, M. and Sakaba, T. (2009). Calcium-dependence of exo- and endocytotic coupling at a glutamatergic synapse. *Neuron* **63**, 216-229.

Huang, J. and Zamponi, G. W. (2017). Regulation of voltage gated calcium channels by GPCRs and post-translational modification. *Curr. Opin. Pharmacol.* **32**, 1-8.

Huntwork, S. and Littleton, J. T. (2007). A complexin fusion clamp regulates spontaneous neurotransmitter release and synaptic growth. *Nat. Neurosci.* **10**, 1235-1237.

Jordán-Álvarez, S., Fouquet, W., Sigrist, S. J. and Acebes, A. (2012). Presynaptic PI3K activity triggers the formation of glutamate receptors at neuromuscular terminals of *Drosophila*. *J. Cell Sci.* **125**, 3621-3629.

Kasprowicz, J., Kuenen, S., Miskiewicz, K., Habets, R. L. P., Smitz, L. and Verstreken, P. (2008). Inactivation of clathrin heavy chain inhibits synaptic recycling but allows bulk membrane uptake. *J. Cell Biol.* **182**, 1007-1016.

Kasprowicz, J., Kuenen, S., Swerts, J., Miskiewicz, K. and Verstreken, P. (2014). Dynamin photoinactivation blocks clathrin and α-adaptin recruitment and induces bulk membrane retrieval. *J. Cell Biol.* **204**, 1141-1156.

Kay, A. R., Alfonso, A., Alford, S., Cline, H. T., Holgado, A. M., Sakmann, B., Snitsarev, V. A., Stricker, T. P., Takahashi, M. and Wu, L.-G. et al. (1999). Imaging synaptic activity in intact brain and slices with FM1-43 in C. elegans, lamprey, and rat. *Neuron* **24**, 809-817.

Klyachko, V. A., Ahern, G. P. and Jackson, M. B. (2001). cGMP-mediated facilitation in nerve terminals by enhancement of the spike afterhyperpolarization. *Neuron* **31**, 1015-1025.

Koenig, J. H. and Ikeda, K. (1989). Disappearance and reformation of synaptic vesicle membrane upon transmitter release observed under reversible blockage of membrane retrieval. *J. Neurosci.* **9**, 3844-3860.

Kohansal-Nodehi, M., Chua, J. J., Urlaub, H., Jahn, R. and Czernik, D. (2016). Analysis of protein phosphorylation in nerve terminal reveals extensive changes in active zone proteins upon exocytosis. *Elife* **5**, e14530.

Krill, J. L. and Dawson-Scully, K. (2016). cGMP-Dependent Protein Kinase Inhibition Extends the Upper Temperature Limit of Stimulus-Evoked Calcium Responses in Motoneuronal Boutons of *Drosophila melanogaster* Larvae. *PLoS ONE* **11**, e0164114.

Krishnamurthy, V. V., Khamo, J. S., Mei, W., Turgeon, A. J., Ashraf, H. M., Mondal, P., Patel, D. B., Risner, N., Cho, E. E., Yang, J. et al. 016). Reversible optogenetic control of kinase activity during differentiation and embryonic development. *Development* **143**, 4085-4094.

Kurdyak, P., Atwood, H. L., Stewart, B. A. and Wu, C.-F. (1994). Differential physiology and morphology of motor axons to ventral longitudinal muscles in larval *Drosophila*. *J. Comp. Neurol.* **350**, 463-472.

Littleton, J. T., Bellen, H. J. and Perin, M. S. (1993). Expression of synaptotagmin in *Drosophila* reveals transport and localization of synaptic vesicles to the synapse. *Development* **118**, 1077-1088.

Luo, C., Gangadharan, V., Bali, K. K., Xie, R.-G., Agarwal, N., Kurejova, M., Tappe-Theodor, A., Tegeder, I., Feil, S., Lewin, G. et al. 012). Presynaptically localized cyclic GMP-dependent protein kinase 1 is a key determinant of spinal synaptic potentiation and pain hypersensitivity. *PLoS Biol.* **10**, e1001283.

Macia, E., Ehrlich, M., Massol, R., Boucrot, E., Brunner, C. and Kirchhausen, T. (2006). Dynasore, a cell-permeable inhibitor of dynamin. *Dev. Cell* **10**, 839-850.

Macleod, G. T., Hegström-Wojtowicz, M., Charlton, M. P. and Atwood, H. L. (2002). Fast calcium signals in *Drosophila* motor neuron terminals. *J. Neurophysiol.* **88**, 2659-2663.

Macleod, G. T., Marin, L., Charlton, M. P. and Atwood, H. L. (2004). Synaptic vesicles: test for a role in presynaptic calcium regulation. *J. Neurosci.* **24**, 2496-2505.

Macleod, G. T., Chen, L., Karunanithi, S., Peloquin, J. B., Atwood, H. L., McRory, J. E., Zamponi, G. W. and Charlton, M. P. (2006). The *Drosophila* cac^{ts2} mutation reduces presynaptic Ca^{2+} entry and defines an important element in $Ca_V2.1$ channel inactivation. *Eur. J. Neurosci.* **23**, 3230-3244.

Marek, K. W. and Davis, G. W. (2002). Transgenically encoded protein photoinactivation (FlAsH-FALI): acute inactivation of synaptotagmin I. *Neuron* **36**, 805-813.

Melom, J. E., Akbergenova, Y., Gavornik, J. P. and Littleton, J. T. (2013). Spontaneous and evoked release are independently regulated at individual active zones. *J. Neurosci.* **33**, 17253-17263.

Meriney, S. D., Gray, D. B. and Pilar, G. R. (1994). Somatostatin-induced inhibition of neuronal Ca^{2+} current modulated by cGMP-dependent protein kinase. *Nature* **369**, 336-339.

O'Banion, C. P., Priestman, M. A., Hughes, R. M., Herring, L. E., Capuzzi, S. J. and Lawrence, D. S. (2018). Design and profiling of a subcellular targeted optogenetic cAMP-dependent protein kinase. *Cell Chem. Biol.* **25**, 100-109.

Osborne, K. A., Robichon, A., Burgess, E., Butland, S., Shaw, R. A., Coulthard, A., Pereira, H. S., Greenspan, R. J. and Sokolowski, M. B. (1997). Natural behavior polymorphism due to a cGMP-dependent protein kinase of *Drosophila*. *Science* **277**, 834-836.

Peng, Q., Wang, Y., Li, M., Yuan, D., Xu, M., Li, C., Gong, Z., Jiao, R. and Liu, L. (2016). cGMP-Dependent protein kinase encoded by *foraging* regulates motor axon guidance in *Drosophila* by suppressing Iola function. *J. Neurosci.* **36**, 4635-4646.

Petrov, A. M., Giniatullin, A. R., Sitdikova, G. F. and Zefirov, A. L. (2008). The role of cGMP-dependent signaling pathway in synaptic vesicle cycle at the frog motor nerve terminals. *J. Neurosci.* **28**, 13216-13222.

Piccioli, Z. D. and Littleton, J. T. (2014). Retrograde BMP signaling modulates rapid activity-dependent synaptic growth via presynaptic LIM kinase regulation of cofilin. *J. Neurosci.* **34**, 4371-4381.

Poskanzer, P. E., Marek, K. W., Sweeney, S. T. and Davis, G. W. (2003). Synaptotagmin I is necessary for compensatory synaptic vesicle endocytosis in vivo. *Nature* **426**, 559-563.

Ramaswami, M., Krishnan, K. S. and Kelly, R. B. (1994). Intermediates in synaptic vesicle recycling revealed by optical imaging of *Drosophila* neuromuscular junctions. *Neuron* **13**, 363-375.
Renger, J. J., Yao, W.-D., Sokolowski, M. B. and Wu, C.-F. (1999). Neuronal polymorphism among natural alleles of a cGMP-dependent kinase gene, *foraging*, in *Drosophila*. *J. Neurosci.* **19**, RC28.
Rieckhof, G. E., Yoshihara, M., Guan, Z. and Littleton, J. T. (2003). Presynaptic N-type calcium channels regulate synaptic growth. *J. Biol. Chem.* **278**, 41099-41108.
Romero-Pozuelo, J., Dason, J. S., Atwood, H. L. and Ferrús, A. (2007). Chronic and Acute Alterations in the Functional Levels of Frequenins 1 and 2 Reveal Their Roles in Synaptic Transmission and Axon Terminal Morphology. *Eur. J. Neurosci.* **26**, 2428-2443.
Romero-Pozuelo, J., Dason, J. S., Mansilla, A., Baños-Mateos, S., Sardina, J. L., Chaves-Sanjuán, A., Jurado-Gómez, J., Santana, E., Atwood, H. L., Hernández-Hernández, Á. et al. (2014). The guanine-exchange factor Ric8a binds to the Ca^{2+} sensor NCS-1 to regulate synapse number and neurotransmitter release. *J. Cell Sci.* **127**, 4246-4259.
Ruth, P., Wang, G. X., Boekhoff, I., May, B., Pfeifer, A., Penner, R., Korth, M., Breer, H. and Hofmann, F. (1993). Transfected cGMP-dependent protein kinase suppresses calcium transients by inhibition of inositol 1,4,5-trisphosphate production. *Proc. Natl. Acad. Sci. USA* **90**, 2623-2627.
Sandoval, A., Duran, P., Gandini, M. A., Andrade, A., Almanza, A., Kaja, S. and Felix, R. (2017). Regulation of L-type CaV1.3 channel activity and insulin secretion by the cGMP-PKG signaling pathway. *Cell Calcium* **66**, 1-9.
Schleede, J. and Blair, S. S. (2015). The Gyc76C receptor guanylyl cyclase and the foraging cGMP-dependent kinase regulate extracellular matrix organization and BMP signaling in the developing wing of Drosophila melanogaster. *PLoS Genet.* **11**, e1005576.
Schlossmann, J., Ammendola, A., Ashman, K., Zong, X., Huber, A., Neubauer, G., Wang, G.-X., Allescher, H. D., Korth, M., Wilm, M. et al. (2000). Regulation of intracellular calcium by a signalling complex of IRAG, IP3 receptor and cGMP kinase Ibeta. *Nature* **404**, 197-201.
Schulte, J., Tepass, U. and Auld, V. J. (2003). Gliotactin, a novel marker of tricellular junctions, is necessary for septate junction development in *Drosophila*. *J. Cell Biol.* **161**, 991-1000.
Sepp, K. J., Schulte, J. and Auld, V. J. (2001). Peripheral glia direct axon guidance across the CNS/PNS transition zone. *Dev. Biol.* **238**, 47-63.
Sild, M., Van Horn, M. R., Schohl, A., Jia, D. and Ruthazer, E. S. (2016). Neural activity-dependent regulation of radial glial filopodial motility is mediated by glial cGMP-dependent protein kinase 1 and contributes to synapse maturation in the developing visual system. *J. Neurosci.* **36**, 5279-5288.
Soykan, T., Maritzen, T. and Haucke, V. (2016). Modes and mechanisms of synaptic vesicle recycling. *Curr. Opin. Neurobiol.* **39**, 17-23.
Spring, A. M., Brusich, D. J. and Frank, C. A. (2016). C-terminal Src kinase gates homeostatic synaptic plasticity and regulates fasciclin ii expression at the *Drosophila* neuromuscular junction. *PLoS Genet.* **12**, e1005886.
Stewart, B. A., Schuster, C. M., Goodman, C. S. and Atwood, H. L. (1996). Homeostasis of synaptic transmission in *Drosophila* with genetically altered nerve terminal morphology. *J. Neurosci.* **16**, 3877-3886.
Sweeney, S. T., Broadie, K., Keane, J., Niemann, H. and O'Kane, C. J. (1995). Targeted expression of tetanus toxin light chain in *Drosophila* specifically eliminates synaptic transmission and causes behavioral defects. *Neuron* **14**, 341-351.
Taoufiq, Z., Eguchi, K. and Takahashi, T. (2013). Rho-kinase accelerates synaptic vesicle endocytosis by linking cyclic GMP-dependent protein kinase activity to phosphatidylinositol-4,5-bisphosphate synthesis. *J. Neurosci.* **33**, 12099-12104.
Tian, A. and Jiang, J. (2014). Intestinal epithelium-derived BMP controls stem cell self-renewal in *Drosophila* adult midgut. *Elife* **3**, e01857.
Turner, K. M., Burgoyne, R. D. and Morgan, A. (1999). Protein phosphorylation and the regulation of synaptic membrane traffic. *Trends Neurosci.* **22**, 459-464.
Vanlandingham, P. A., Barmchi, M. P., Royer, S., Green, R., Bao, H., Reist, N. and Zhang, B. (2014). AP180 couples protein retrieval to clathrin-mediated endocytosis of synaptic vesicles. *Traffic* **15**, 433-450.
Venken, K. J. T., Kasprowicz, J., Kuenen, S., Yan, J., Hassan, B. A. and Verstreken, P. (2008). Recombineering-mediated tagging of *Drosophila* genomic constructs for *in vivo* localization and acute protein inactivation. *Nucleic Acids Res.* **36**, e114.
Verstreken, P., Ohyama, T. and Bellen, H. J. (2008). FM 1-43 labeling of synaptic vesicle pools at the *Drosophila* neuromuscular junction. *Methods Mol. Biol.* **440**, 349-369.
Verstreken, P., Ohyama, T., Haueter, C., Habets, R. L., Lin, Y. Q., Swan, L. E., Ly, C. V., Venken, K. J., De Camilli, P. and Bellen, H. J. (2009). Tweek, an evolutionarily conserved protein, is required for synaptic vesicle recycling. *Neuron* **63**, 203-215.
Wagh, D. A., Rasse, T. M., Asan, E., Hofbauer, A., Schwenkert, I., Durrbeck, H., Buchner, S., Dabauvalle, M. C., Schmidt, M., Qin, G. et al. (2006). Bruchpilot, a protein with homology to ELKS/CAST, is required for structural integrity and function of synaptic active zones in *Drosophila*. *Neuron* **49**, 833-844.
Warming, S., Costantino, N., Court, D. L., Jenkins, N. A. and Copeland, N. G. (2005). Simple and highly efficient BAC recombineering using galK selection. *Nucleic Acids Res.* **33**, e36.
Wei, J.-Y., Jin, X., Cohen, E. D., Daw, N. W. and Barnstable, C. J. (2002). cGMP-induced presynaptic depression and postsynaptic facilitation at glutamatergic synapses in visual cortex. *Brain Res.* **927**, 42-54.
Willmott, N. J., Wong, K. and Strong, A. J. (2000). A fundamental role for the nitric oxide-G-kinase signaling pathway in mediating intercellular Ca(2+) waves in glia. *J. Neurosci.* **20**, 1767-1779.
Wodarz, A., Hinz, U., Engelbert, M. and Knust, E. (1995). Expression of crumbs confers apical character on plasma membrane domains of ectodermal epithelia of *Drosophila*. *Cell* **82**, 67-76.
Wu, L.-G., Hamid, E., Shin, W. and Chiang, H.-C. (2014). Exocytosis and endocytosis: modes, functions, and coupling mechanisms. *Annu. Rev. Physiol.* **76**, 301-331.
Xu, J., Luo, F., Zhang, Z., Xue, L., Wu, X.-S., Chiang, H.-C., Shin, W. and Wu, L.-G. (2013). SNARE proteins synaptobrevin, SNAP-25, and syntaxin are involved in rapid and slow endocytosis at synapses. *Cell Reports* **3**, 1414-1421.
Yao, J., Kwon, S. E., Gaffaney, J. D., Dunning, F. M. and Chapman, E. R. (2012). Uncoupling the roles of synaptotagmin I during endo- and exocytosis of synaptic vesicles. *Nat. Neurosci.* **15**, 243-249.
Yawo, H. (1999). Involvement of cGMP-dependent protein kinase in adrenergic potentiation of transmitter release from the calyx-type presynaptic terminal. *J. Neurosci.* **19**, 5293-5300.
Yoshimura, N., Seki, S. and de Groat, W. C. (2001). Nitric oxide modulates Ca(2+) channels in dorsal root ganglion neurons innervating rat urinary bladder. *J. Neurophysiol.* **86**, 304-311.
Zhang, Z., Wang, D., Sun, T., Xu, J., Chiang, H. C., Shin, W. and Wu, L. G. (2013). The SNARE proteins SNAP25 and synaptobrevin are involved in endocytosis at hippocampal synapses. *J. Neurosci.* **33**, 9169-9175.
Zhao, G., Wu, Y., Du, L., Li, W., Xiong, Y., Yao, A., Wang, Q. and Zhang, Y. Q. (2015). *Drosophila* S6 Kinase like inhibits neuromuscular junction growth by downregulating the BMP receptor thickveins. *PLoS Genet.* **11**, e1004984.
Zhou, X.-B., Arntz, C., Kamm, S., Motejlek, K., Sausbier, U., Wang, G.-X., Ruth, P. and Korth, M. (2001). A molecular switch for specific stimulation of the BKCa channel by cGMP and cAMP kinase. *J. Biol. Chem.* **276**, 43239-43245.
Zucker, R. S. and Regehr, W. G. (2002). Short-term synaptic plasticity. *Annu. Rev. Physiol.* **64**, 355-405.

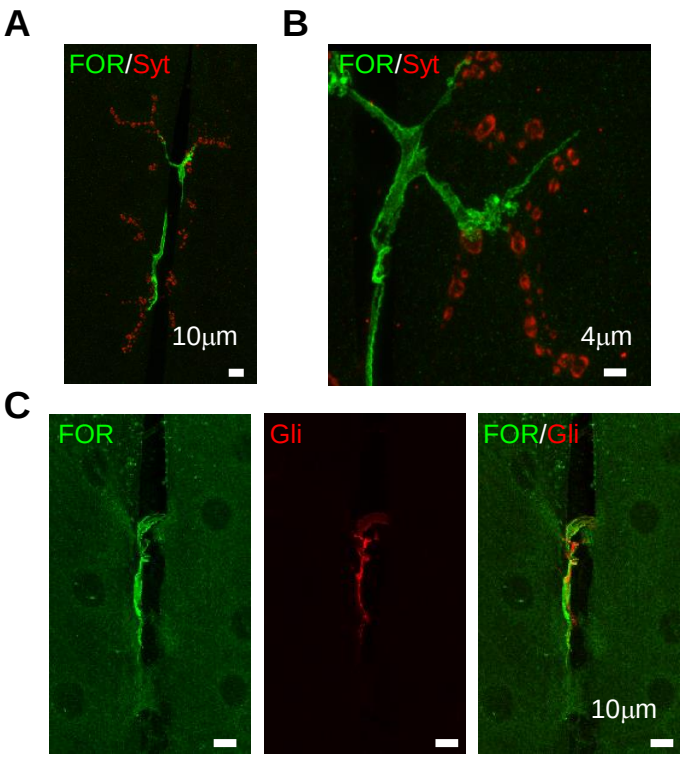

Figure S1. *for* is expressed in glia at the larval neuromuscular junction. A, B, Representative images of third instar larval neuromuscular junctions. *for* expression was inferred by using a for^{pr3}-*GAL4* to drive mCD8-GFP. Preparations were then stained with anti-GFP (green) and anti-Synaptotagmin (red). C, Preparations were stained with anti-GFP (green) and anti-Gliotactin (red). mCD8-GFP driven by for^{pr3}-*GAL4* colocalizes with the glial marker, Gliotactin.

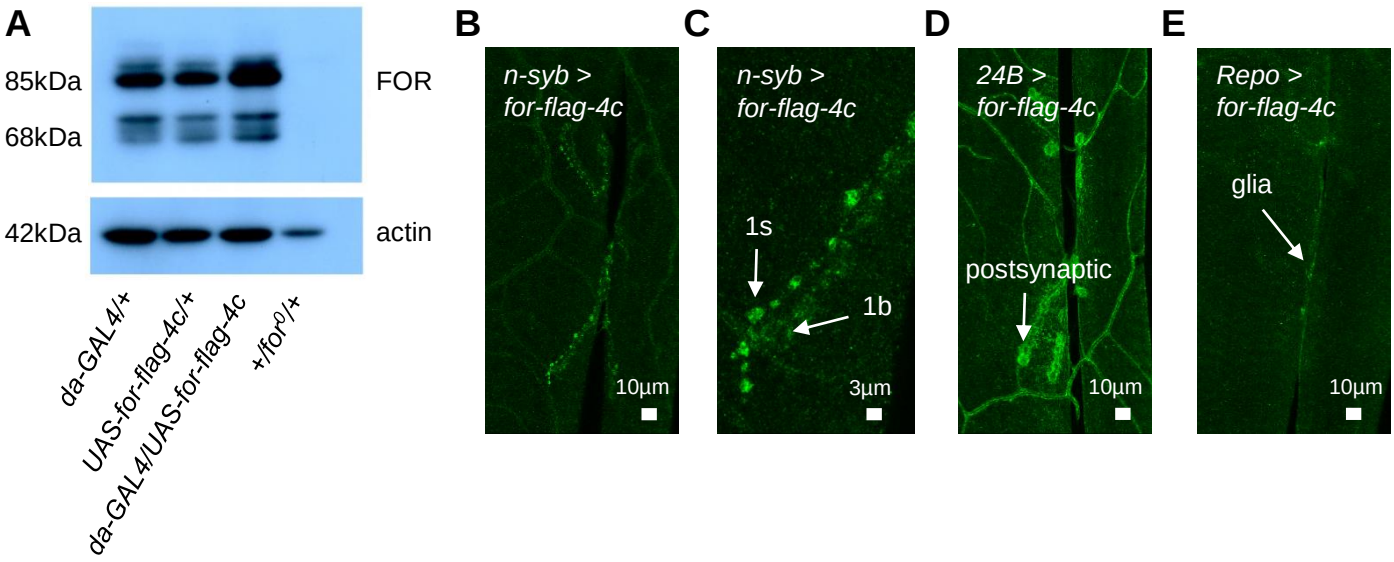

Figure S2. Tissue specific expression of FOR-flag-4c. ***A***, Western blot of whole larval homogenates of the GAL4 control (*+;+;da-GAL4/+*), UAS control *(+;+;UAS-for-flag-4c/+*) and experimental (*+;+;+da-GAL4/UAS-for-flag-4c*) genotypes. ***B***,***C***,***D***,***E*** Representative images of fixed third instar larval nmjs stained with an anti-flag antibody. ***B***,***C***, FOR-flag-4c expressed presynaptically, in both 1b and 1s boutons (indicated by arrows). ***D***, FOR-flag-4c expressed at postsynaptic sites (indicated by arrows). ***E***, FOR-flag-4c expressed in glia (indicated by arrows).

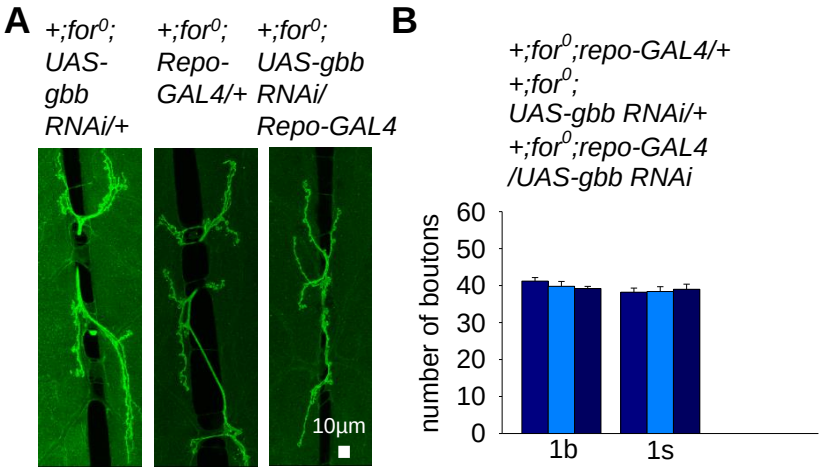

Figure S3. Reducing glial Gbb does not rescue the increased nerve terminal growth seen in *for*^{0} null mutants. ***A***, Fixed larval nmjs stained with FITC-conjugated anti-HRP antibody. ***B***, The increased number of 1b and 1s boutons seen in the *for*^{0} null mutant was not rescued by knocking down *gbb* in glia (*+;for*^{0}*;UAS-gbb-RNAi/Repo-GAL4*; P>0.05 for 1b and 1s boutons; n=5). Values represent the mean ±sem. Significance was determined using a one-way ANOVA test.

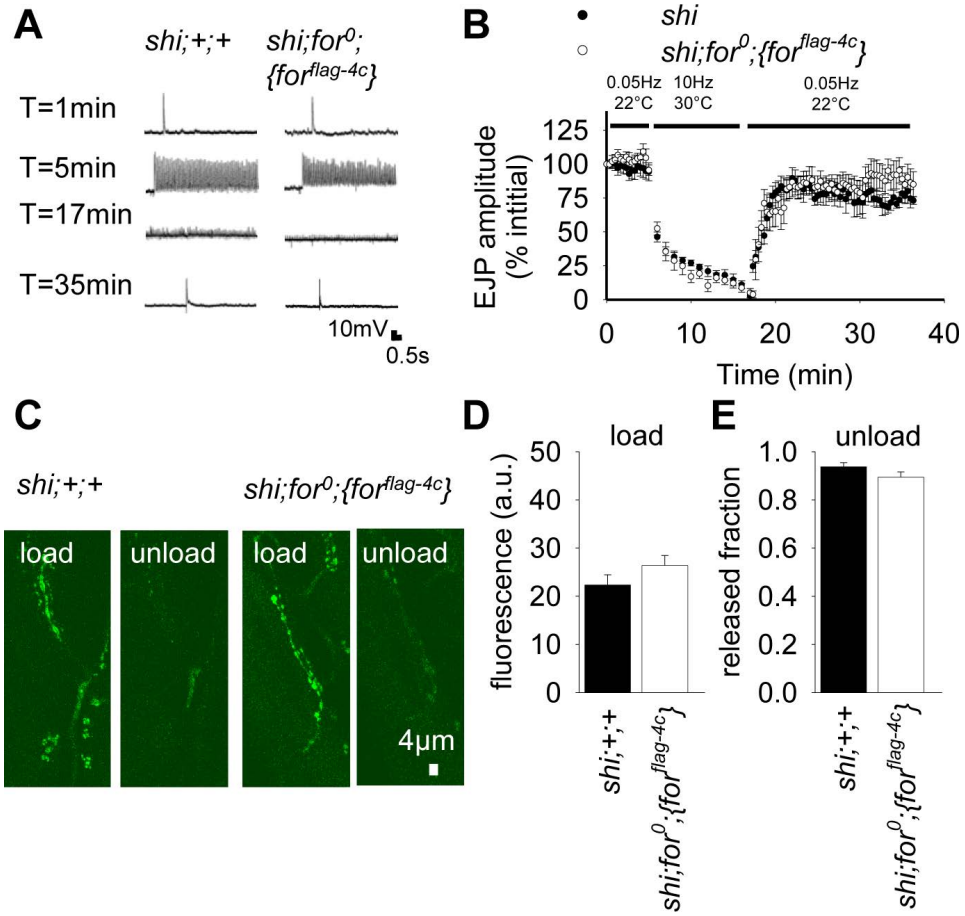

Figure S4. Synaptic transmission and SV recycling is normal in the absence of FlAsH-FALI in *shi;for^{0};{for$^{flag\text{-}4c}$}* nmjs. ***A***, Representative traces of EJPs. Preparations were maintained in HL6 (1mM Ca^{2+}) saline. The segmental nerve was stimulated at 0.05Hz for 5min at 22°C, followed by 10Hz stimulation for 12min at 30°C, and then stimulated at 0.05Hz for 20min at 22°C to assess recovery of synaptic transmission. ***B***, There was no significant differences in recovery of synaptic transmission between *shi;+;+* and *shi;for^{0};{for$^{flag\text{-}4c}$}* genotypes (P>0.05; n=7). ***C***, Representative images of preparations that were stimulated (90mM K^{+} for 10min) at 30°C to trap SVs. Endocytosis was assayed by incubating preparations with 10μM FM4-64 for 20min at 22°C (load), then washing in 0mM Ca^{2+} HL6 (with 75μM Advasep-7 for first 2min) for 10min to remove extracellular FM4-64 and fluorescence (F) was then measured. 90mM K^{+} saline was reapplied for 10min to cause unloading and F measured again (unload). ***D***, There was no significant differences in FM4-64 loading between *shi;+;+* and *shi;for^{0};{for$^{flag\text{-}4c}$}* genotypes (P=0.2034; n=6). ***E***, A similar fraction of FM4-64 was released, demonstrating that recycled SVs could undergo exocytosis (P=0.1560; n=6). Values represent the mean ±sem. Significance was determined using unpaired t-tests.